Cyclophilin A and Nuclear Factor of Activated T Cells Are Essential in Cyclosporine-Mediated Suppression of Polyomavirus BK Replication

Y. J. Li[a,b], H. H. Wu[a,b], C. H. Weng[a,b],
Y. C. Chen[a], C. C. Hung[a], C. W. Yang[a],
R. Y. L. Wang[c], N. Sakamoto[d] and Y. C. Tian[a,*]

[a] Kidney Research Center, Department of Nephrology,
Chang Gung Memorial Hospital, Taipei, Taiwan and Chang
Gung University, Tao Yuan, Taiwan
[b] Graduate Institute of Clinical Medical Sciences, Chang
Gung University, Taiwan
[c] Department of Biomedical Sciences, Chang Gung
University, Tao Yuan, Taiwan
[d] Department of Gastroenterology and Hepatology, Tokyo
Medical and Dental University, Tokyo, Japan
*Corresponding author: Ya-Chung Tian,
dryctian@adm.cgmh.org.tw

[Correction made after online publication May 29, 2012:
author affiliations have been updated.]

Immunosuppressants have impacts on the development of polyomavirus-associated nephropathy. We previously demonstrated that cyclosporin A (CsA) suppressed polyomavirus BK (BKV) replication. The role of cyclophilin A (CypA) and nuclear factor of activated T cells (NFAT) in CsA-imposed suppression of BKV replication was determined in this study. Results demonstrated that knockdown of CypA but not CypB significantly reduced BKV large T antigen (TAg) expression and BKV titer. Overexpression of CypA reversed CypA siRNA-induced inhibition in BKV TAg expression. In addition, CypA overexpression attenuated the suppressive effect of CsA on TAg expression, suggesting CypA implicated in CsA-mediated anti-BKV effect. Knockdown of NFATc3 abrogated TAg expression, while overexpression of NFATc3 promoted TAg expression and augmented BKV promoter activity. NFATc3 binding to the BKV promoter was verified by chromatin immunoprecipitation assay and electrophoretic mobility shift assay. Renal histology also displayed an increase in NFATc3 expression in tubulointerstitium of BKV-associated nephropathy. Furthermore, overexpression of NFATc3 rescued CsA-mediated inhibition of BKV load and TAg expression. A CsA analog, NIM811, which cannot block NFAT functionality, failed to suppress TAg expression. In conclusion, CypA and NFAT are indispensable in BKV replication. CsA inhibits BKV replication through CypA and NFAT, which may be potential targets of anti-BKV treatment.

Key words: Cyclophilin, cyclosporine, nuclear factor of activated T cell, polyomavirus BK

Introduction

Polyomavirus BK (BKV) reactivation in renal transplant patients is a critical problem (1,2). It has been reported that 5–10% of the subjects develop polyomavirus-associated nephropathy (PVAN) (3) and up to 50% of the patients with PVAN eventually lose their allograft within 2–3 years (4). Tacrolimus and mycophenolate are associated with a higher incidence of PVAN compared with other immunosuppressants (5, 6). Cyclosporin A (CsA), a calcineurin inhibitor, has been commonly used for the prevention of allograft rejection after organ transplantation due to its selective function in inhibiting T cell immunity. In addition to immunosuppression, CsA can also inhibit replication of various viruses, including human immunodeficiency virus (HIV) type I, vaccinia virus, herpes simplex virus, hepatitis C virurs (HCV) and cytomegalovirus (CMV) (7–12). It has been reported that CsA can inhibit BKV replication in green monkey kidney cells (Vero E6 cells) (13). Similarly, we previously demonstrated that CsA suppressed BKV replication and its noncoding control region (NCCR) promoter activity in cultured human renal proximal tubular cells (14). Nevertheless, the mechanisms by which CsA inhibits BKV replication remain elusive.

Cyclophilin A (CypA) was isolated as a CsA-specific binding protein by Handschumacher et al. in 1984 (15). To date, seven major cyclophilin (Cyp) members including CypA, CypB, CypC, CypD, CypE, Cyp40 and CypNK have been identified in humans (16). CsA binds to cyclophilins to form a complex and subsequently inhibits phosphatase activity that is required for calcineurin activation. Through inhibition of calcineurin activation, CsA induces phosphorylation of nuclear factor of activated T cells (NFAT), which prevents translocation of NFAT from the cytoplasm into the nucleus, thereby blocking NFAT activity (17,18). Five NFAT

2348

family members have been identified to date. Of these, NFATc1 (NFAT2), NFATc2 (NFAT1), NFATc3 (NFAT4) and NFATc4 (NFAT3) are dephosphorylated and activated by calcineurin, while they are phosphorylated and inactivated by CsA (19,20).

Cyp and NFAT, two CsA mediators, have been shown to play important roles in CsA-induced suppression of different viral replication. For example, CsA inhibits mouse CMV and HCV replications via a CypA-dependent pathway (11,21). In addition, NFAT can enhance HIV-1 replication in primary human CD4 T cells (22). In this study, we demonstrated that CypA and NFATc3 are essential for CsA-mediated suppression of BKV replication. This study may provide a new therapeutic target for the treatment of BKV infection.

Materials and Methods

Materials and cell culture

Mouse anti-SV40 TAg antibody, which can also recognize BKV TAg, was purchased from Calbiochem (La Jolla, CA, USA). Anti-BKV VP1 antibody was the gift of Abnova Co. (Taipei, Taiwan). Antiflag antibody and CsA were purchased from Sigma (Sigma Chemical Company Ltd., Poole, UK). CypA, CypB and NFATc3 siRNA were obtained from Dharmacon Inc. (Lafayette, CO, USA). Goat anti-NFATc3 antibody was purchased from R&D Systems (Minneapolis, MN, USA) and rabbit anti-NFATc4 antibodies were purchased from Santa Cruz Biotech, Inc. (Santa Cruz, CA, USA).

Immortalized human renal proximal tubular cells, HK-2, were cultured as described previously (23).

Flag-epitope (DYKDDDDK) cDNA was attached to the full-length coding sequences of CypA, CypB, NFATc3 and NFATc4, which are obtained by qPCR from human genomic DNA using the standard technique (24).

Real-time quantitative polymerase chain reaction (qPCR)

qPCR was performed as described previously (25). Briefly, total RNA was isolated from cells and reverse-transcribed to DNA. qPCR was performed according to the manufacturer's instructions using an ABI-Prism 7700 with SYBR Green I (PE-Applied Biosystems, Cheshire, UK, Britain). Primers used to assay BKV TAg and glyceraldehyde-3-phosphate dehydrogenase (GAPDH) transcript levels (BKV TAg: 5-CTGTCCCTAAAACCCTGCAA-3 and 5- GCCTTTCCTTCCATTCAACA -3; GAPDH: 5-TTCCAGGAGCGAGATCCCT-3 and 3-CACCCATGACGAACATGGG-5) were constructed to be compatible with a single reverse transcription-PCR thermal profile (95°C for 10 min, 40 cycles of 95°C for 30 s and 60°C for 1 min). Experimental results are presented as the transcript level of the analyzed genes relative to GAPDH transcript level.

To determine viral load, BKV and cellular DNA were extracted from cell lysate using a QIAamp® DNA Mini Kit (Qiagen, Hilden, Germany). qPCR was performed as described above. The BKV DNA was normalized by analyzing samples in parallel by the quantitative PCR for the cellular tubulin β2A DNA using the commercial primers and probes (Hs00742533_s1*, probe: GTCCTCAAGCATGGTCTTTCTACTT; Applied Biosystems).

Gene silencing by short interfering RNA (siRNA)

RNA interference was used to reduce CypA, CypB and NFATc3 expressions. Briefly, 0.5–1.5 μg of siRNA against CypA, CypB, NFATc3 or control siRNA

was diluted in the serum-free medium to give a final volume of 100 μL. Subsequently, RNAiFectl transfection reagent was mixed with diluted siRNA at ratio from 6:1 to 3:1. Following incubation for 15 min at room temperature, the mixture was added to the culture medium.

Luciferase assay

The NCCR of the BKV and BKV TAg were constructed as described previously (14). The BKV NCCR in early and late orientation was used in this study. Luciferase assays utilized the Dual-Luciferase Report Assay (Promega, Madison, WI, USA) applied according to the manufacturer's recommendations. Luciferase activity was measured using a luminometer (MLX micro titer plate luminometer, Dynex Ltd., Chantilly, VA, USA) and examined on duplicates of each sample. Experimental results were presented as firefly luciferase activity normalized to Renilla luciferase activity.

Western blot analysis

Total cellular protein extraction was performed as described previously (26). Protein samples mixed with reducing SDS sample buffer were resolved on a 10% SDS-PAGE and then electroblotted. Nonspecific binding was blocked with a 5% nonfat milk solution. The membrane was then incubated with primary antibody overnight at 4°C followed by incubation with a horseradish peroxidase (HRP) conjugated secondary antibody. Proteins were visualized using enhanced chemiluminescence (Amersham Biosciences, Amersham, UK). Protein bands of Western blot analysis were quantified using Quantity One software (BioRad). The density of each protein band was normalized with that of tubulin.

Chromatin immunoprecipitation

DNA was cross-linked with 1% formaldehyde at 37°C for 10 min and cells were then resuspended in a SDS lysis buffer. Cell lysate was sonicated and supernatants were diluted 10-fold in a ChIP dilution buffer and precleared with salmon sperm DNA/protein A agarose 50% slurry (Millipore, Billerica, MA, USA). Following brief centrifugation, the supernatant fraction was immunoprecipitated with rabbit anti-NFATc3 or anti-NFATc4 overnight. After the addition of protein A agarose slurry, samples were incubated for 1 h at 4°C. Pellet agarose was washed once with wash buffer I (Millipore, Billerica, USA) and buffer II (Millipore, Billerica, MA, USA). DNA was eluted in 1% SDS, 0.1 M NaHCO3 at room temperature for 1 h. Following proteinase K digestion, DNA was recovered with phenol/chloroform extraction and ethanol precipitation. After the addition of glycogen, DNA was amplified by qPCR using SYBR Green Master Mix as described above. Primers were designed for the BKV NCCR as follows: forward 5'-GCAAAAATTGCAAAAGAATAGG-3' and reverse 5'-TTCCAGTCCAGGTTTTACCAA-3'.

Electrophoretic mobility shift assay

Electrophoretic mobility shift assay (EMSA) was employed for the analysis of NCCR DNA binding ability by the purified recombinant NFATc3 and NFATc4 protein. Briefly, the pGEX vector for expression in BL21 (DE3) Escherichia coli (Merck) was used to produce the GST-tagged recombinant proteins. Proteins were over-expressed through induction with 0.2 mM Isopropyl β-D-1-thiogalactopyranoside (IPTG) at 16°C for 10 h. Both of the recombinant NFATc3 and NFATc4 were purified through affinity chromatography. For NFAT-DNA binding followed by EMSA, essentially a 20 μL reaction comprised of purified protein, ^{32}p-labelled double-stranded DNA (BKV NCCR) and 125 μg/uL poly dl-dC buffered in 12 mM HEPES pH 7.8, 75 mM KCl, 1 mM EDTA, 4 mM GTP and 12.5% glycerol was incubated at room temperature for 1 h. The protein–DNA mixtures were subsequently loaded onto a 6% DNA Retardation Gel (Invitrogen) alongside "no protein" and "no DNA" controls, and migrated in a 0.5 × TBE running buffer for 1.5 h. Competition experiments were performed with 100-fold excess of the respective unlabelled probes.

Viral progeny

Viral progeny is measured as described by Moriyama et al. (27). Briefly, infected cells were extracted and lysates were undiluted or diluted to 1:10 or 1:100 and then seeded on cells in 8-well chamber slides for 72 h. Cells were then fixed with 3% paraformaldehyde and permeabilized with 0.2% Triton in PBS. Subsequently, cells were incubated with the mouse anti-SV40 TAg antibody overnight and then incubated with FITC-conjugated antibody at for 1 h. Slides were finally mounted using the Vectashield mounting medium (Vector Laboratories) containing 4′,6′-diamidino-2-phenylindole (dapi) (Molecular Probes, California, USA) to stain nuclei. The fluorescence-forming unit was calculated according to the protocol (27).

Immunohistochemistry

Under permission of the ethics committee of our hospital, residual renal biopsy specimens obtained from 2 PVAN patients were analyzed for deposition of NFATc3 and TAg expressions. Normal tissue away from the edge of renal cell carcinoma (RCC) obtained from one RCC patient undergoing nephrectomy was used as a negative control. Kidney specimens were fixed with 4% paraformaldehyde and embedded in paraffin. Following deparaffinization, sections were then immersed in 3% H_2O_2 in methanol and blocked with 5% bovine albumin/PBS for 20 min. Following incubation with anti-NFATc3 or anti-SV40 TAg for 1 h, sections were treated with relevant biotin-conjugated antibodies and the NFATc3 or TAg immunostaining was then displayed using a Vectastain ABC kit (Vector Laboratories).

Statistical analysis

All the data were presented as means ± SEM. Statistical analysis was performed using the unpaired Student's t-test. A value of $p < 0.05$ was considered to represent a significant difference.

Results

### Inhibition of CypA but not CypB expression reduced BKV replication

To determine whether CypA is required in BKV (TU strain) replication, endogenous CypA expression was knocked down by gene silencing. Inhibition of CypA expression by CypA siRNA was confirmed by Western blot analysis which showed a significant decrease in CypA protein expression (Figure 1A). Blockade of CypA expression led to a reduction in BKV TAg expression (Figure 1A). Similarly, inhibition of CypA expression resulted in a decrease in the level of TAg transcripts as determined by qPCR (Figure 1B).

To assess whether CypA knockdown-mediated inhibition of BKV replication could be rescued by reintroduction of CypA into cells, endogenous CypA expression was suppressed using CypA siRNA followed by CypA overexpression. Following inhibition of CypA expression, BKV TAg expression was suppressed while BKV TAg expression was enhanced after the reintroduction of CypA into cells (Figure 2A). Similarly, the results of qPCR also confirmed that the reintroduction of CypA into cells led to an increase in the level of TAg transcripts (Figure 2B) and viral load (Figure 2C). To measure the infectious progeny, viral lysates were collected at the end of the experiments and seeded on the new cells for 72 h. The result confirmed that knockdown of
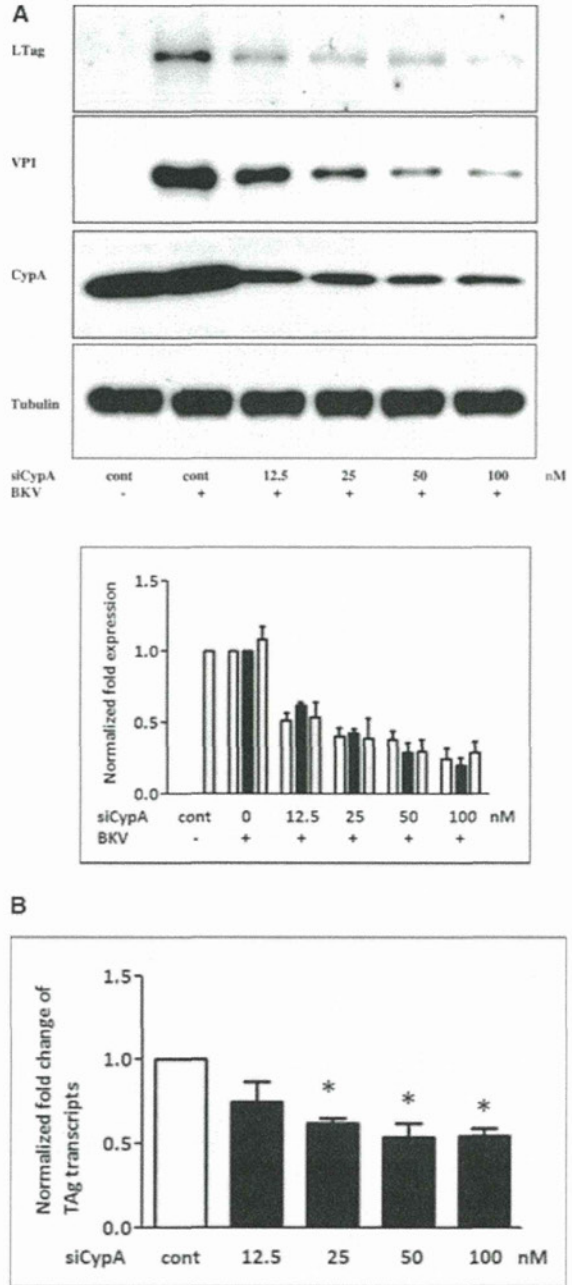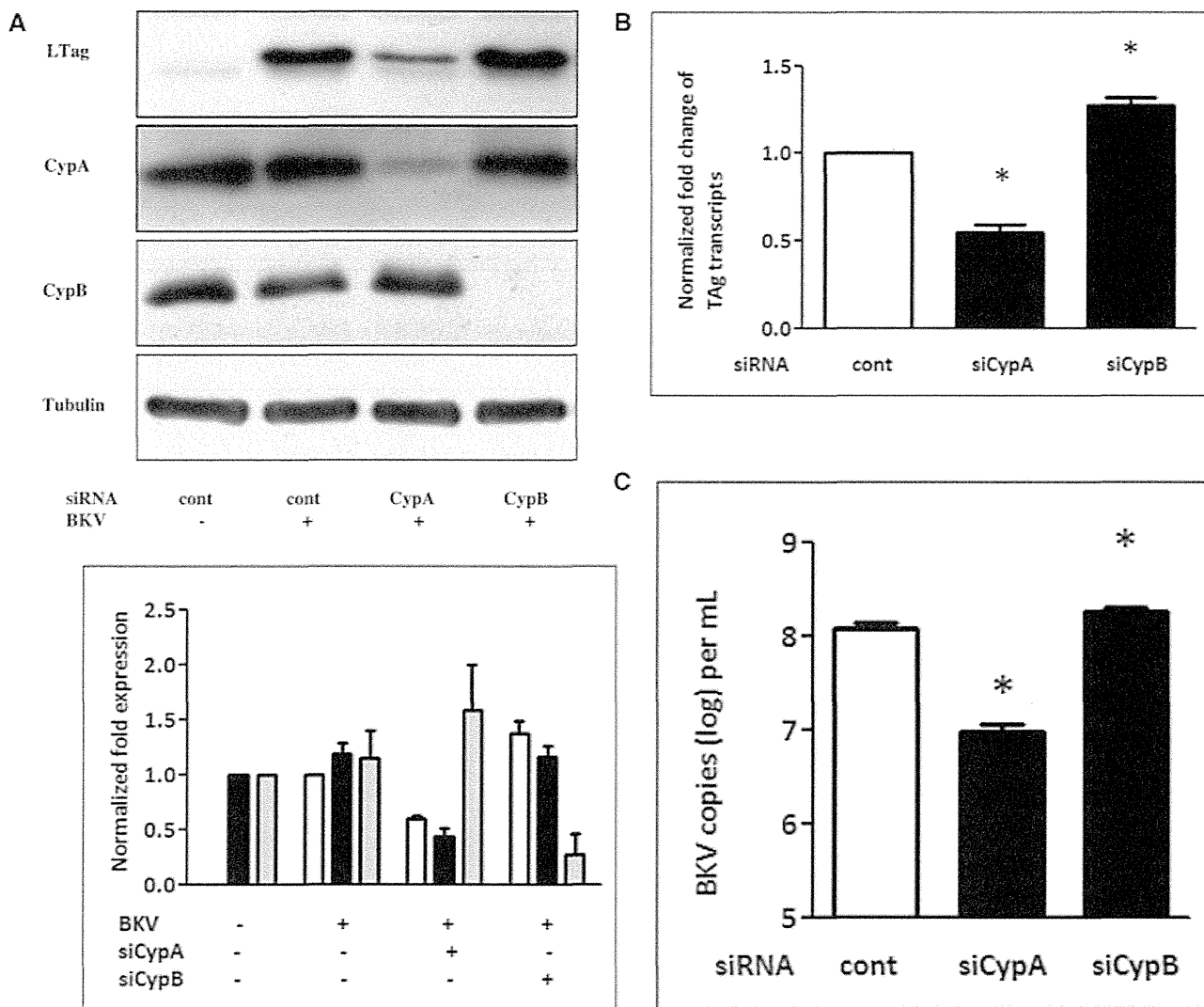

Figure 1: Inhibition of CypA reduced BKV TAg expression. HK-2 cells were transfected with siCypA at different concentrations (12.5–100 nM) overnight. Cells were then infected with the BKV (1.0×10^6 copies/mL) for further 72 h under serum-free condition. Cells transfected with scramble siRNA as the control (100 nM). Cell lysate was subjected to Western blot analysis to determine BKV TAg expression (A) or qPCR to assess the levels of BKV TAg transcripts (B). The density of each protein band (TAg: white bar, VP1: black bar, CypA: gray bar) was normalized with that of tubulin and the fold changes compared to the control were displayed in the lower panel. One representative result of Western blot analysis from three individual replicate experiments is shown. Results of qPCR are expressed as the relative fold increase of TAg transcripts over that of the control, which is arbitrarily set to one (*$p < 0.05$).
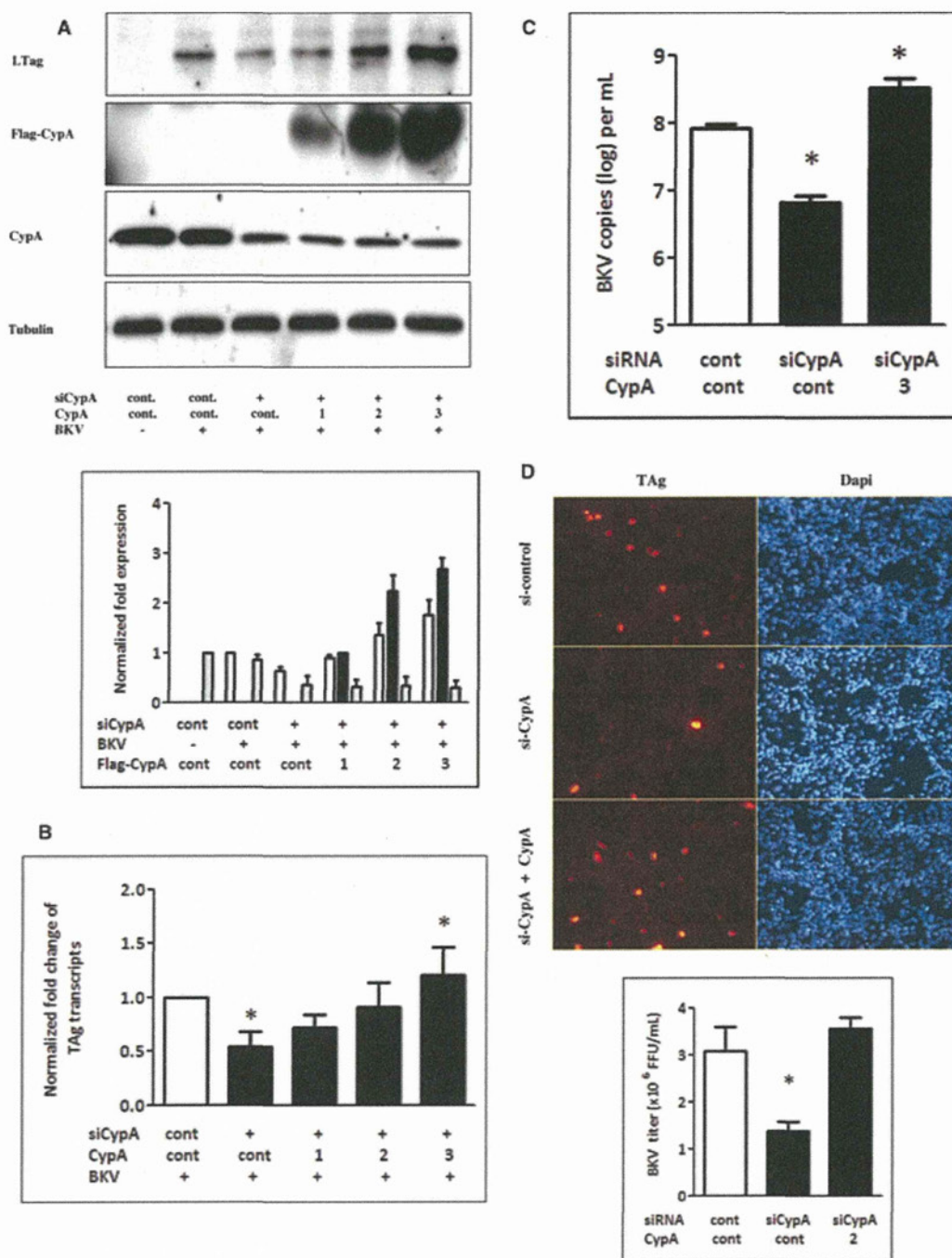
Figure 2: CypA knockdown-induced suppression of BKV TAg expression was rescued by reintroduction of CypA. Cells were transfected with CypA siRNA (50 nM) or scramble siRNA (control) overnight and washed with medium followed by transfection with different concentrations (1–3 μg/mL) of plasmids expressing flag-tagged CypA or an empty control vector. Cells were then infected with the BKV (1.0×10^6 copies/mL) for further 72 h. Cell lysate was subjected to Western blot analysis to determine BKV TAg expression (A) or qPCR to assess the levels of BKV TAg transcripts (B) and viral load. (C) The density of each protein band (TAg: white bar, Flag-tagged CypA: black bar, endogenous CypA: gray bar) was normalized with that of tubulin and the fold changes compared to the control were displayed in the lower panel. For unknown reasons, the flag-tagged CypA expression was unable to be detected by anti-CypA antibody. Results of qPCR are expressed as the relative fold increase of TAg transcripts over that of the control, which is arbitrarily set to one. (*$p < 0.05$ vs. control). (D) At the end of the experiments performed under the above condition, viral lysates were collected and seeded on the new cells for 72 h. Intracellular viral load was then determined by counting the TAg immunostaining-positive cells (upper panel) to calculate fluorescence-forming units (FFU) as described in the Materials and Methods section.

Figure 3: Inhibition of CypA but not CypB reduced BKV TAg expression. Cells were transfected with siCypA or siCypB (50 nM) overnight. Cells were then infected with the BKV (1.0 × 10^{6} copies/mL) for further 72 h under serum-free condition. Cells transfected with scramble siRNA as the control. Cell lysate was subjected to Western blot analysis to determine BKV TAg expression (A) or qPCR to assess the levels of BKV TAg transcripts (B) and viral load (C). The density of each protein band (TAg: white bar, CypA: black bar, CypB: gray bar) was normalized with that of tubulin and the fold changes compared to the control were displayed in the lower panel. Results of qPCR are expressed as the relative fold increase of TAg transcripts over that of the control, which is arbitrarily set to one ($^*p < 0.05$).

CypA reduced BKV load and the reintroduction of exogenous CypA restored this inhibition (Figure 2D).

In addition to CypA, it has been reported that CypB is also required for viral replication (28, 29). To establish whether CypB participates in BKV replication, endogenous CypB expression was inhibited by CypB siRNA. Western blot analysis showed that, in contrast to CypA, knockdown of CypB slightly increased BKV TAg expression (Figure 3A). Similarly, inhibition of CypB expression slightly enhanced the level of TAg transcripts (Figure 3B) and viral load (Figure 3C). These results suggest an indispensable role of CypA but not CypB in BKV replication.

CypA overexpression attenuated CsA-mediated suppression of BKV replication

To assess whether CypA is crucial in CsA-mediated inhibition of BKV replication, cells were transfected with the CypA-expressing plasmids followed by administration of CsA for 72 h. In accordance with our previous study (14), administration of CsA (1 μg/mL) resulted in a reduction in BKV TAg expression. Importantly, overexpression of CypA significantly attenuated CsA-mediated inhibition in BKV TAg expression compared with transfection of the control vector (Figure 4). At high CypA expression levels, CypA overexpression even surpassed the CsA-mediated inhibitory effect

2352

LTag						
Flag-CyPA						
Tubulin						

CsA	-	-	+	+	+	+
CypA	cont.	cont.	cont.	1	2	3
BKV	-	+	+	+	+	+
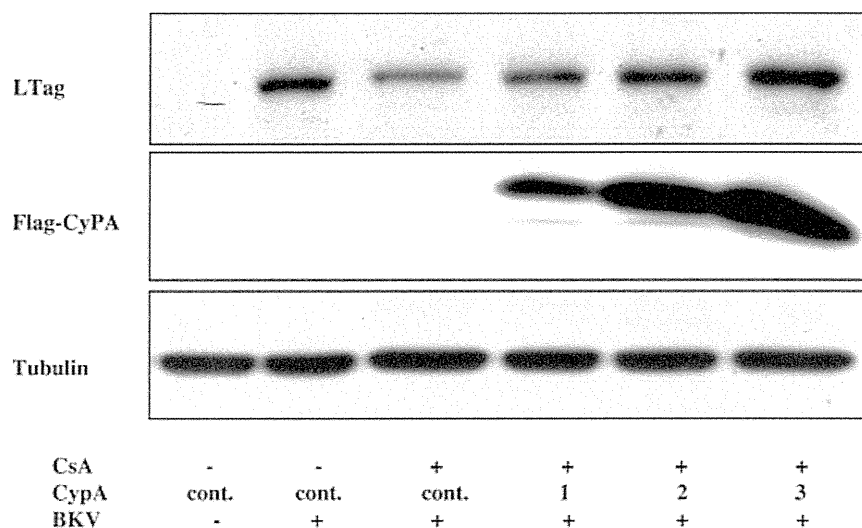
Figure 4: The suppressive effect of CsA on BKV TAg expression was attenuated by overexpression of CypA. Cells were transfected with different concentrations (1–3 µg/mL) of plasmids expressing flag-tagged CypA or an empty control vector. Cells were then infected with the BKV (1.0 × 10^6 copies/mL) in the presence or absence of CsA (1 µg/mL) under serumfree condition for 72 h. Cell lysate was subjected to Western blot analysis to determine BKV TAg expression (A) or BKV DNA copies (B). The density of each protein band (TAg: white bar, flagtagged CypA: black bar) was normalized with that of tubulin and the fold changes compared to the control were displayed in the lower panel. One experiment representative of three individual replicate experiments is shown.
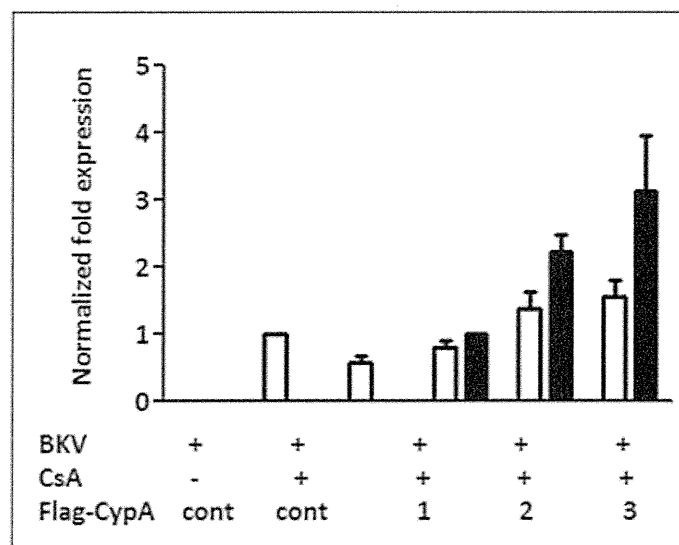

and led to a significant enhancement in BKV TAg expression.

NFAT is crucial for BKV replication

Since NFAT is a major downstream transcription factor of the cyclophilin/calcineurin complex (30), we therefore assessed whether NFAT plays a role in BKV replication. Results demonstrated that NFATc3 and NFATc4 were prominently expressed in HK-2 cells, whereas NFATc1 and NFATc2 were weakly detected in cells (data not shown). To clarify the effect of NFATc3 and NFATc4 on BKV replication, NFATc3 or NFATc4 was overexpressed overnight, followed by addition of BKV to cells. The result demonstrated that overexpression of NFATc3 enhanced BKV TAg expression (Figure 5A). Similarly, NFATc4 overexpression

also facilitated BKV TAg expression (Figure 5B). These results indicate that there is a stimulatory effect of NFATc3 and NFATc4 on BKV replication.

BKV NCCR is the main regulatory region of BKV replication. To assess whether NFAT can regulate BKV NCCR, plasmids expressing NFATc3 or NFATc4 and the BKV NCCR luciferase reporter in early or late orientation were cotransfected in cells. NFATc3 or NFATc4 overexpression led to an increase in promoter activity of the BKV NCCR luciferase reporter in early orientation, reaching a 2.9- or 3.4-fold increase respectively when compared with that of the mock transfection (Figure 5C). Similarly, the activity of the late NCCR promoter reporter was increased 2.5- or 2.7-fold, respectively, by NFATc3 or NFATc4 overexpression (Figure 5D).
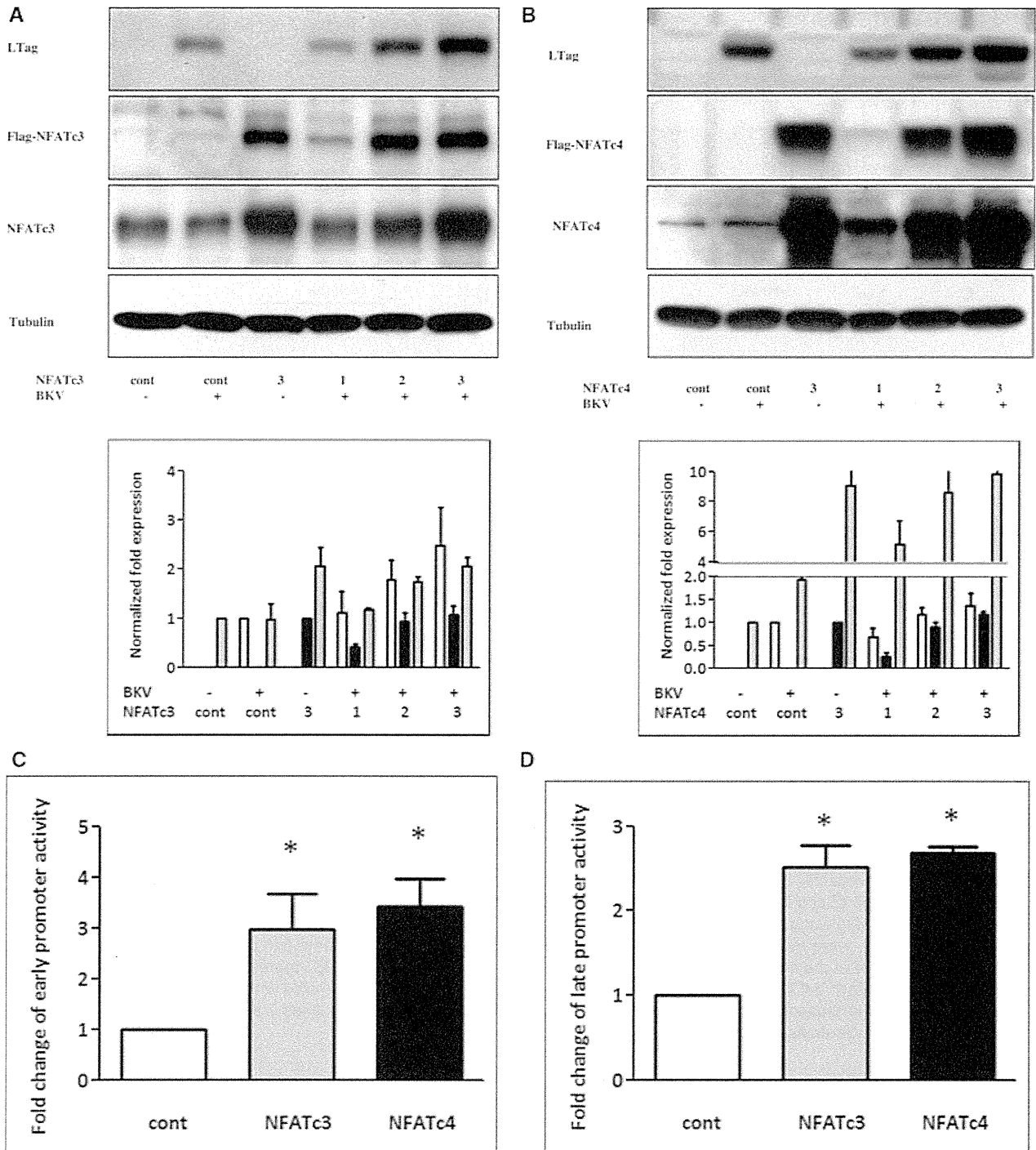
Figure 5: NFAT overexpression enhanced BKV TAg and the BKV NCCR activity. (A and B) Cells were transfected with plasmids expressing NFATc3 (A) or NFATc4 (B) overnight and then infected with the BKV (1.0×10^6 copies/mL) for further 72 h. Cell lysate was subjected to Western blot analysis to determine BKV TAg expression. The density of each protein band (TAg: white bar, flag-tagged NFATc3 or NFATc4: black bar; total NFATc3 or NFATc4: gray bar) was normalized with that of tubulin and the fold changes compared to the control were displayed in the lower panel. (C and D) The NCCR firefly luciferase reporter vector (1 μg/mL) in early (C) or late orientation (D), the *Renilla* luciferase vector (1 μg/mL), the plasmids expressing NFATc3 (3 μg/mL) (gray bar) or NFATc4 (3 μg/mL) (black bar) or the control vector (white bar) were cotransfected into HK-2 cells overnight. Cells were grown under serum-free condition for further 48 h. Luciferase assays were then performed on duplicate samples and the firefly luciferase activity was normalized to that of *Renilla* luciferase activity. The results were obtained from four independent experiments (*$p < 0.05$).
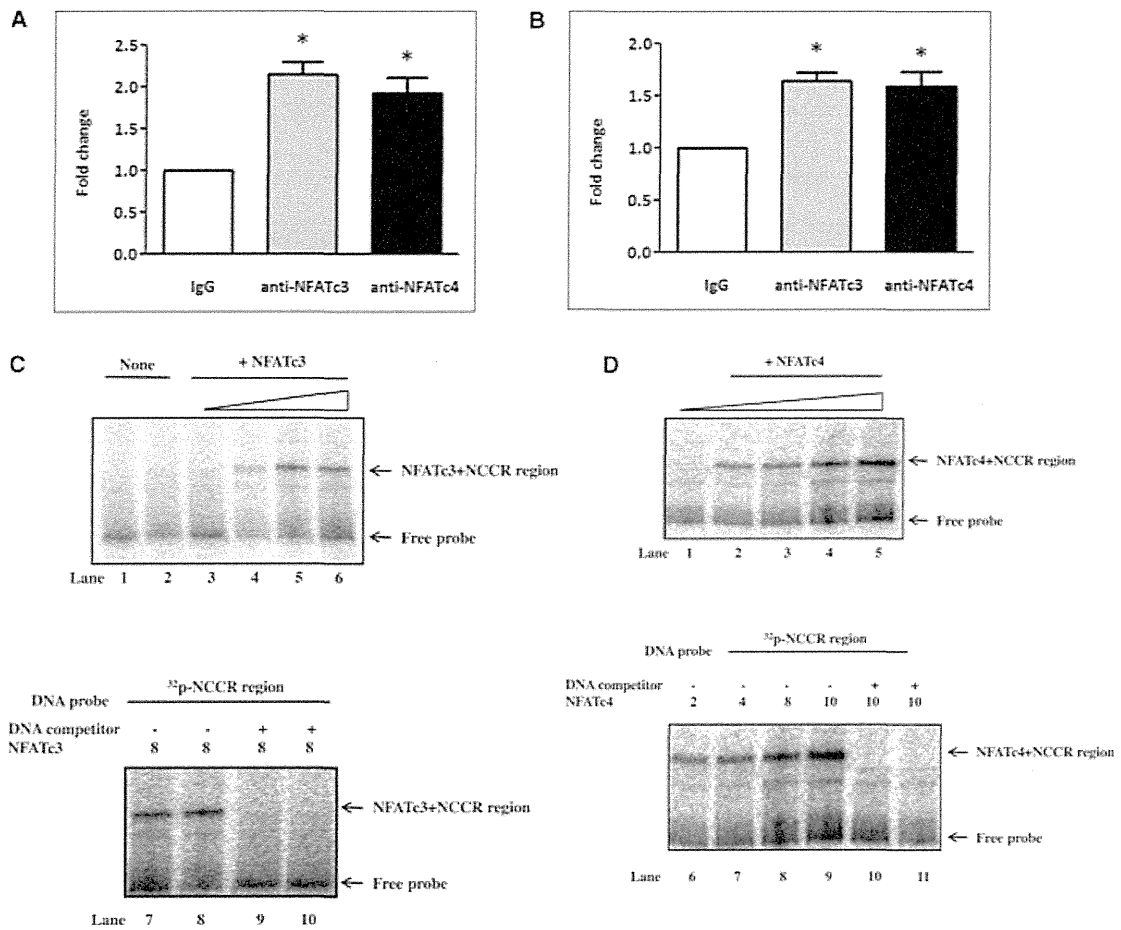
Figure 6: NFAT binds to the BKV promoter. (A and B) Cells were transfected with the plasmids expressing the BKV NCCR (A) or infected with BKV (1.0×10^6 copies/mL) (B) for 48 h. Cells were then subjected to the ChIP assay described in the Materials and Methods section. Immunoprecipitated DNA by anti-NFATc3 (gray bar), anti-NFATc4 (black bar) or a nonspecific IgG antibody (white bar) was quantified by qPCR using primers detecting the BKV NCCR. Results are expressed as the relative fold increase of the NFATc3 or NFATc4-associated DNA over that of the nonspecific IgG control, which is arbitrarily set to one. All data are represented as mean ± SE from four independent experiments (*$p < 0.05$). (C and D) Interaction of NFATc3, NFATc4 with BKV noncoding control region was assessed by EMSA. Binding complexes were separated using 6% nondenaturing PAGE as described in the Materials and Methods section. Labeled double-stranded oligonucleotides, NCCR, were mixed with purified recombinant NFATc3 (C) in the final concentration of 0, 2, 4, 8 μg/μL (lanes 3 and 6) and recombinant NFATc4 in the final concentration of 0, 2, 4, 8, 10 μg/μL (D: lanes 1 and 5). GST protein was used for a negative control shown as 'none' (C: lanes 1 and 2). In the parallel experiments, NCCR oligonucleotides were mixed with 8 μg/μL of purified recombinant NFATc3 or NFATc4 in the presence (C: lanes 9 and 10; D: lanes 10 and 11) or absence (C: lanes 7 and 8; D: lanes 6 and 9) of 100× unlabeled NCCR oligonucleotides as competitors.

To assess whether NFAT can bind to the BKV promoter, cells were transfected with the plasmids expressing BKV NCCR (Figure 6A) or infected with BKV (Figure 6B) for 48 h and chromatin was then immunoprecipitated with anti-NFATc3 or anti-NFATc4 antibody followed by qPCR to quantify the binding of the viral promoter to NFATc3 or NFATc4. Results of the ChIP assay demonstrated that the levels of the BKV promoter DNA binding to NFATc3 and NFATc4 were increased 2.1- and 1.9-fold, respectively, by transfection with the plasmids expressing BKV NCCR or increased 1.6- and 1.5-fold respectively by BKV infection when compared to that of the DNA immunoprecipitated with a nonspecific IgG antibody (Figures 6A and B). To sup-

port the results of the ChIP assay, we performed EMSA by in vitro mixture of recombinant NFATc3 or NFATc4 proteins and [32]p-labelled double-stranded DNA (BKV NCCR) prior to gel shift analysis. Results clearly demonstrated an increase in binding of NFATc3- (Figure 6C) and NFATc4 (Figure 6D) with BKV NCCR.

To further verify the role of NFAT in BKV replication, NFATc3 expression was suppressed by NFATc3 siRNA and cells were then infected with BKV. Western blot analysis showed that knockdown of NFATc3 expression reduced BKV TAg expressions (Figure 7A). Similarly, knockdown of NFATc3 by siRNA also reduced the promoter activity of

A

B
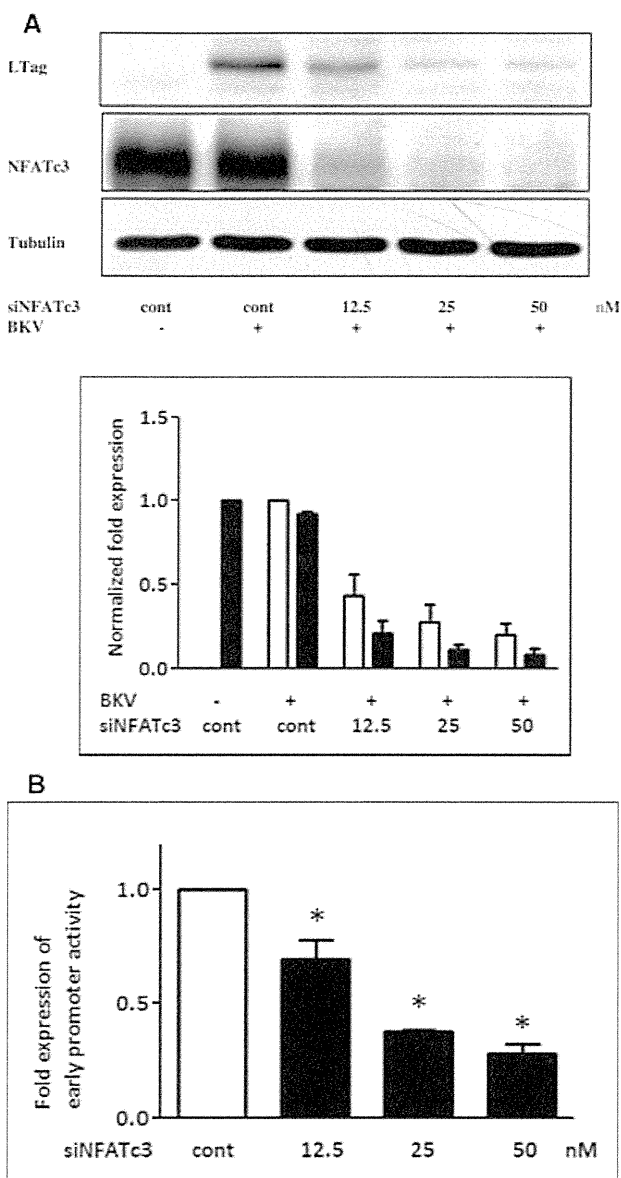
Figure 7: Inhibition of NFATc3 reduced BKV TAg expression.
(A) Cells were transfected with NFATc3 siRNA at different concentrations (12.5–50 nM) overnight. Cells were then infected with the BKV (1.0 × 10^6 copies/mL) for further 72 h under serum-free condition. Cells were transfected with scramble siRNA as the control (50 nM). Cell lysate was subjected to Western blot analysis to determine BKV TAg expression. The density of each protein band (TAg: white bar, NFATc3: black bar) was normalized with that of tubulin and the fold changes compared to the control were displayed in the lower panel. One representative result of Western blot analysis from three individual replicate experiments is shown. (B) Cells were transfected with NFATc3 siRNA at different concentrations (12.5–50 nM) or scramble siRNA overnight. The NCCR firefly luciferase reporter plasmid and the *Renilla* luciferase plasmid were cotransfected into HK-2 cells for further 48 h. The firefly luciferase activity was normalized to that of *Renilla* luciferase activity. The results were obtained from three independent experiments (*p <0.05 vs. the control).

the BKV NCCR luciferase reporter (Figure 7B). These data confirm that NFAT are essential for BKV replication.

CsA-mediated inhibition of BKV replication was rescued by NFAT overexpression

CsA inhibits calcineurin activity and causes NFAT phosphorylation that inactivates NFATs and prevents subsequent nuclear translocation to trigger transcription of target genes in immune cells (31). To appreciate whether CsA can cause NFATc3 phosphorylation and then inactivate NFATc3 in HK-2 cells, CsA was added to HK-2 cells for 24 h. NIM811, a CsA derivative, which cannot inhibit calcineurin activity and cause NFAT activation, was used as a control. The results revealed that the administration of CsA led to slow migration of NFATc3, indicating phosphorylation and inactivation of NFATc3 activity by CsA (Figure 8A). In contrast, the addition of NIM811 did not result in slow migration of NFATc3, implying the lack of an inhibitory effect on NFATc3 activity. Interestingly, while CsA suppressed BKV TAg expression, NIM811 did not alter BKV TAg expression (Figure 8A). This result suggests that NFATc3 activity is implicated in CsA-mediated suppression of BKV replication.

To verify the crucial role of NFATc3 in CsA-imposed suppression of BKV replication, NFATc3 was overexpressed in the presence of CsA. Western blot analysis showed that NFATc3 or NFATc4 overexpression diminished the inhibitory effect of CsA on BKV TAg expressions, while overexpression of the control vector did not reverse CsA-mediated inhibition of BKV TAg expression (Figures 8B and C) and viral load (Figure 8D). In addition, NFATc3 or NFATc4 overexpression even surpassed the CsA-induced reduction in the BKV early promoter activity (Figure 8E). These results suggest that NFAT is essential mediators in CsA-mediated suppression of BKV replication.

NFAT expression is increased in PVAN

Since NFAT is crucial for BKV replication, NFATc3/NFATc4 expression in renal biopsy specimen obtained from two patients with PVAN was assessed. Results of immunohistochemistry revealed that NFATc3/NFATc4 staining was prominently increased in the cytoplasm and nuclei of renal tubules and interstitial lymphocytes in the kidney of PVAN (Figures 9B and F; NFATc4 staining: not shown) when compared with that of the normal control (Figures 9A and E). PVAN was confirmed as BKV TAg expression was detected in the tubules (Figures 9D and G).

Discussion

In this study, we demonstrate the importance of cyclophilin in regulation of both BKV early and late replication in HK-2 cells as knockdown of CypA-inhibited BKV LTag and VP1 expression. While CypA knockdown substantially suppressed BKV LTag and VP1 expressions, knockdown of CypB did not prominently affect BKV LTag and VP1 expression. Cyclophilins have been identified to play a crucial role in HIV

2356
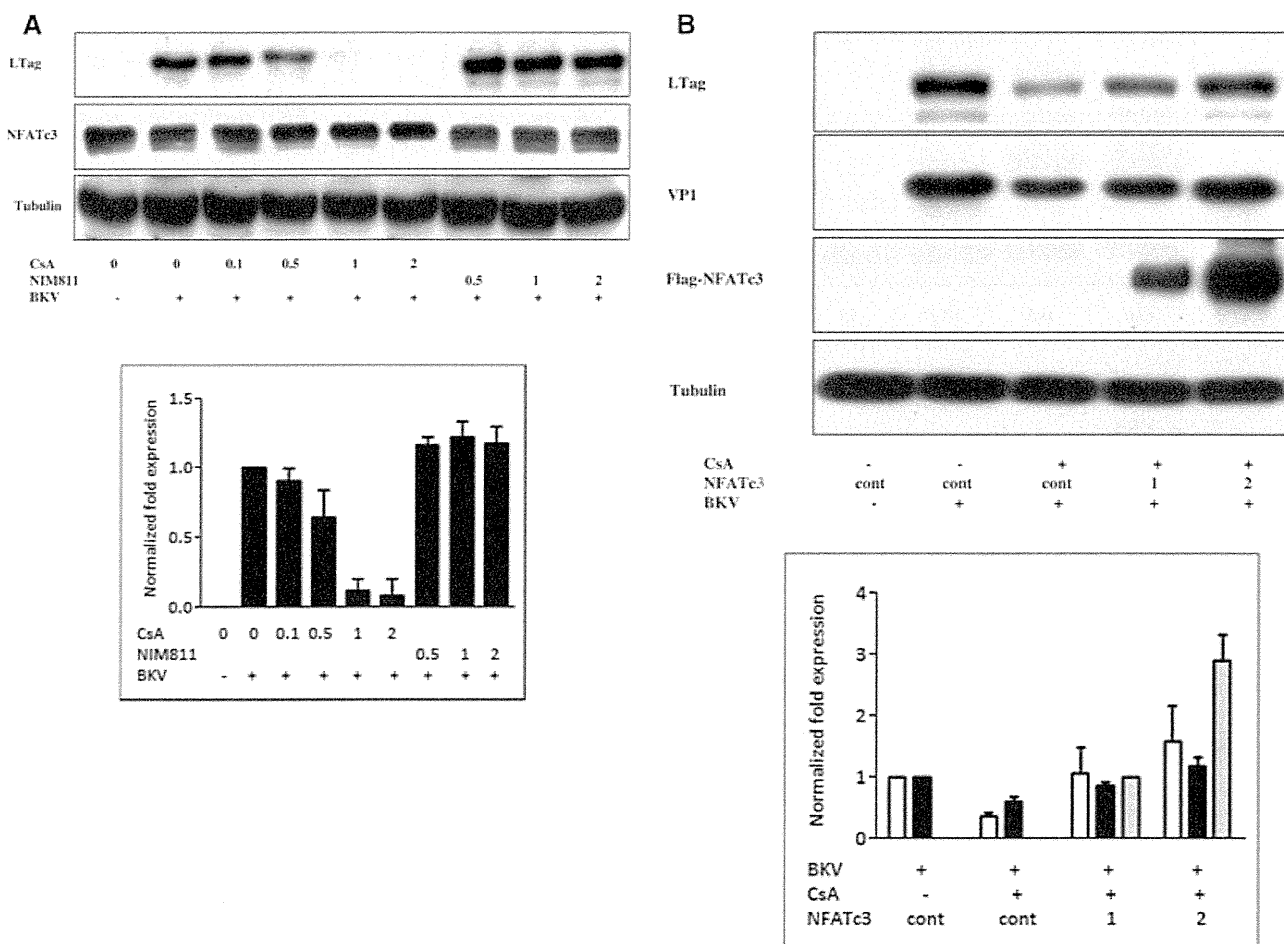
Figure 8: The suppressive effect of CsA on BKV TAg expression was attenuated by overexpression of NFATs. (A) Cells were infected with the BKV (1.0 × 10⁶ copies/mL) in the presence or absence of CsA (0.5–2 μg/mL) or NIM811 (0.5–2 μg/mL) for 72 h. Cell lysate was subjected to Western blot analysis to determine NFATc3 and BKV TAg expression. (B and C) Cells were transfected with different concentrations (1–2 μg/mL) of plasmids expressing flag-tagged NFATc3 (B) or NFATc4 (C) or an empty control vector overnight. Cells were then infected with the BKV (1.0 × 10⁶ copies/mL) in the presence or absence of CsA (1 μg/mL) under serum-free condition for 72 h. Cell lysate was subjected to Western blot analysis to determine BKV TAg expression or to qPCR for viral load (D). The density of each protein band (TAg: white bar, VP1: black bar, Flag-NFATc3/c4: gray bar) was normalized with that of tubulin and the fold-changes compared to the control were displayed in the lower panel. One experiment representative of three individual replicate experiments is shown. (E) The NCCR early promoter firefly luciferase reporter (1 μg/mL), the Renilla luciferase vector (1 μg/mL), the plasmids expressing NFATc3 (3 μg/mL) (gray bar) or NFATc4 (3 μg/mL) (black bar) or the control vector (white bar) were cotransfected into HK-2 cells overnight. Cells were incubated in the presence or absence of CsA (1 μg/mL) for further 48 h. The firefly luciferase activity was normalized to that of Renilla luciferase activity. The results were obtained from four independent experiments. (*p <0.05 vs. the control, #p<0.05 vs. the CsA group).

and HCV replication (7,28,32–35). Watashi et al. have found that inhibition of either CypA or CypB expression suppresses HCV replication (12,28). In contrast, Yang et al. have recently revealed that knockdown of CypA, but not of CypB and CypC expression reduces HCV replication (35). Our study suggests that CypA is the principle cyclophilin member for regulation of BKV replication in renal proximal tubular cells.

We demonstrated that knockdown of NFATc3 abrogated BKV TAg expression and reduced the BKV early promoter

activity. In addition, overexpression of either NFATc3 or NFATc4 promoted BKV TAg expression and augmented BKV NCCR early and late promoter activity. Furthermore, NFATc3 and NFATc4 binding to the BKV promoter was verified by the ChIP assay and EMSA. Our results substantiate a critical role of NFAT for BKV TU strain replication. Interestingly, Jordan et al. recently discovered three NFAT binding sites on the promoter of the BKV Dunlop strain (36). They demonstrate that overexpression of NFATc3 or NFATc4 in Vero cells augments the viral promoter activity. Mutational analysis reveals that these binding sites are essential for
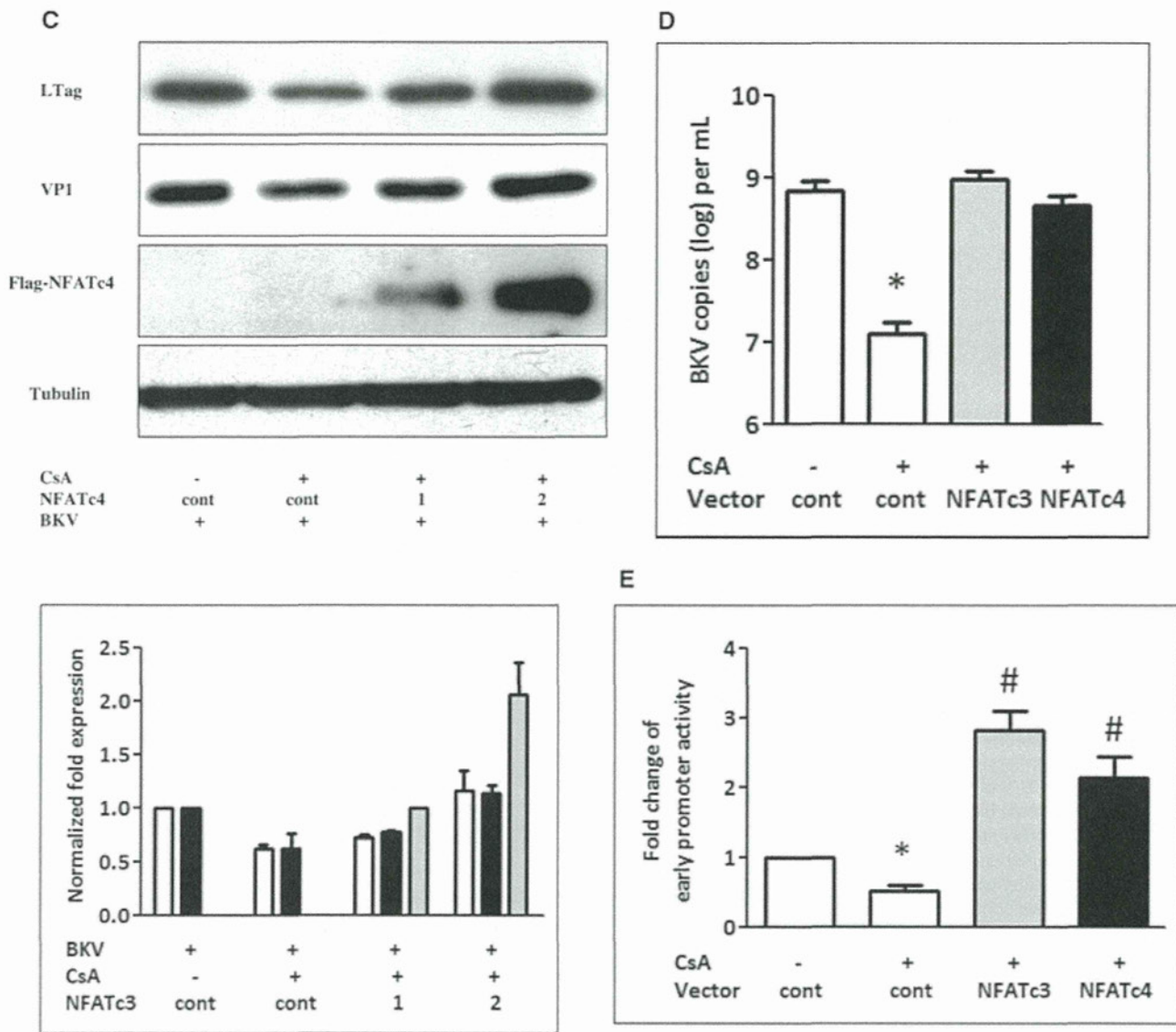
Figure 8: Continued

regulation of BKV transcription. The essential role of NFAT in viral replication has been reported in other viruses. Romanchikova et al. showed that NFATc1 and NFATc2 binding to HIV LTR enhanced HIV replication (37). Manley et al. have shown that NFATc3 is indispensable in JC virus (JCV) infection in glial cells as inhibition of NFATc3 by a NFAT peptide inhibitor reduced JCV promoter activity (38). In this study, renal histology of PVAN displayed an increase of NFATc3/c4 expression in renal tubules and lymphocytes. We speculate that increased NFATc3 expression in renal tubules may augment BKV replication and enhance the development of PVAN.

Previously we have shown that CsA can suppress BKV replication as the addition of CsA to the BKV-infected cells reduces BKV LTag expression (14). In this study, we further demonstrated that overexpression of CypA attenuated the suppressive effect of CsA on BKV TAg expression, which suggests anti-BKV effect of CsA requires inhibition of CypA activity. Several studies have demonstrated the essential role of cyclophilins in CsA-imposed inhibition of viral replication. Nakagawa et al. show that inhibition of HCV replication by CsA is through blockade of the activities of cyclophilins including CypA, CypB and CypC (29). Yang et al. also identified that CypA plays an essential
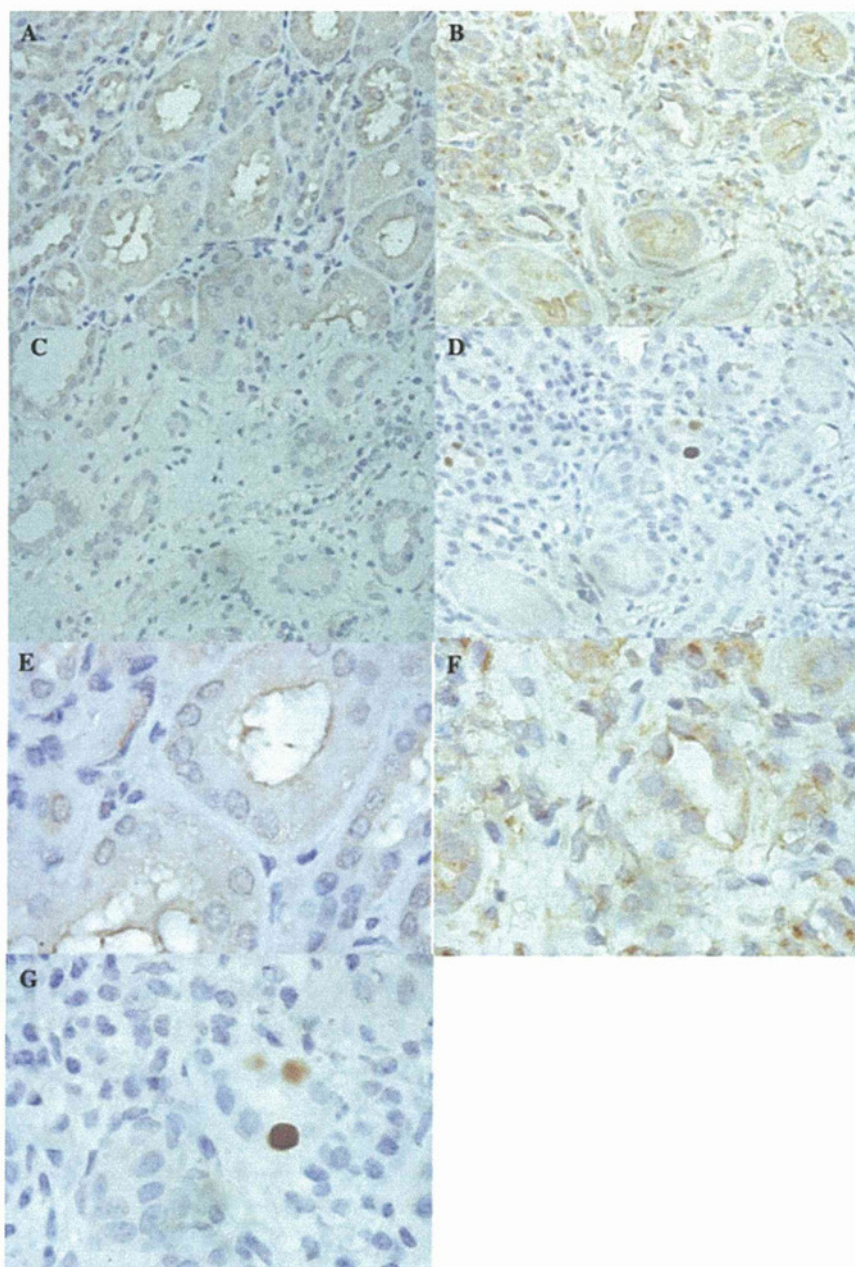
Figure 9: NFATc3 expression is increased in PVAN. NFATc3 expression (B and F, brown staining) and BKV TAg expression (D and G, dark brown staining) in the renal biopsy specimen obtained from PVAN patients were assessed by immunohistochemistry described in the Materials and Methods section. A negative control of the same specimen was performed using only the secondary antibody with omission of the primary antibody (anti-NFATc3) (C). Normal tissues cut from residual kidney specimen obtained from a nephrectomized patient with renal cell carcinoma were used as the control and stained for NFATc3 expression (A and E). Magnification: ABCD 400×, EFG 1000×.

role in CsA-resistant HCV infection (35). CypA is also a critical mediator in CsA-associated suppression of HIV, as the inhibitory effect of CsA on HIV replication results from CsA-induced disruption of the interaction between HIV Gag polyprotein and CypA (7). In accordance with these findings from other viruses, our results also suggest that CypA is critical for CsA-mediated suppression of BKV replication.

In this study, CsA, which caused phosphorylation of NFAT and inhibited NFAT activation, similar to the finding in COS-7 cells (39), suppressed BKV replication. In contrast, NIM811, which did not affect phosphorylation of NFAT and block NFAT functionality, failed to suppress BKV replication. Importantly, the overexpression of NFATc3 or NFATc4 attenuated the CsA-mediated inhibitory effect on BKV TAg expression. Moreover, NFATc3 or NFATc4 overexpression even surpassed the CsA-imposed reduction in the BKV early promoter activity. These findings indicate that NFAT is essential for the CsA-associated anti-BKV effect. It has been documented that CsA substantially interferes with the transcriptional activity of HIV mediated by NFAT in human CD4 T cells (22). Manely et al. report that CsA suppresses human polyomavirus JC (JCV) replication through
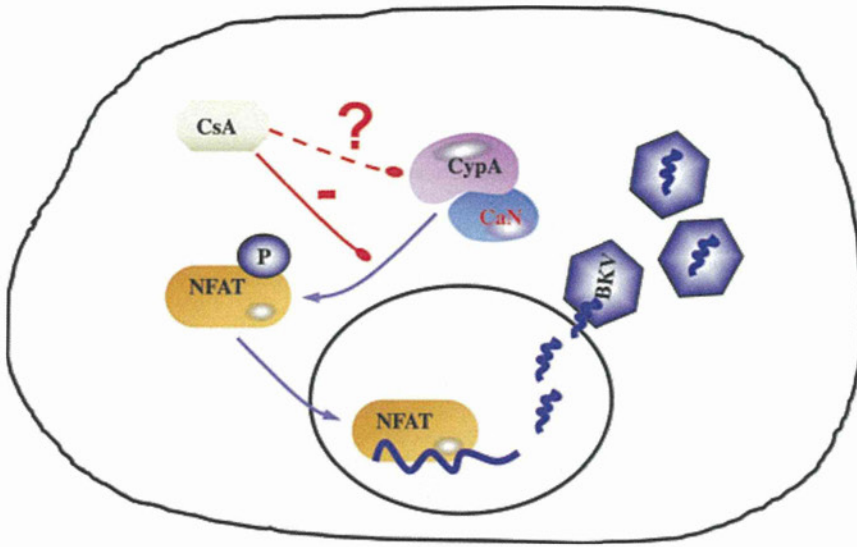
Figure 10: Schematic summary depicts a proposed mechanism of the inhibitory effect of CsA on BKV replication. NFATc3/c4, the calcineurin downstream mediator, can bind to the BKV NCCR to promoter viral replication. Administration of CsA blocks endogenous CypA/CaN function and leads to inhibition of dephosphorylation of NFAT, thus inhibiting NFAT functionality and preventing NFAT-mediated enhancement of BKV replication; CaN = calcineurin; CsA = cyclosporin; CypA = cyclophilin A; NFAT= nuclear factor of activated T cells.

blockade of NFAT4 activation (38). They identify a NFAT binding site as an enhancer in the early region of the JCV promoter, which is also conserved in the BKV promoter (38). In contrast, Jordan et al. identify three NFAT binding sites (GGAAA) in the triplicate P regions of the BKV Dunlop promoter and two of these are potential repressors (36). The BKV archetype strain also has three NFAT binding sites in the P, Q and R regions. Compared to the BKV archetype stain, the BKV TU strain has the rearranged NCCR containing the intact P- and Q-regions followed by a partial depletion of the R region and a duplication of a partial P–Q–R region (40). However, we also find three NFAT binding sites in the P, Q and R regions of the BKV TU promoter. Interestingly, despite the rearrangement of BKV NCCR, BKV archetype, Dunlop and TU strains all have three NFAT binding sites. Just which NFAT binding sites are the main regulatory sites in CsA-mediated suppression of BKV replication requires further elucidation.

The proposed mechanism regarding how CsA suppresses BKV replication is summarized in Figure 10. CypA is required in CsA-imposed inhibition of BKV replication since CypA overexpression can rescue this inhibitory response. In addition, NFATc3/c4, the calcineurin downstream mediator, can bind to the BKV NCCR to promoter viral replication. CsA, which blocks calcineurin activity, causes inhibition of dephosphorylation of NFAT, thus inhibiting NFAT functionality and preventing NFAT-mediated enhancement of BKV replication. Nevertheless, unlike CsA, knockdown of the CypA expression did not affect dephosphorylation of NFATc3 and the binding of NFATc3 to the BKV NCCR was not altered by administration of CypA siRNA (data not shown), suggesting an NFAT-independent role of CypA in BKV replication. Whether CsA also affects the CypA-dependent but NFAT-independent pathway (dash line in Figure 10) to regulate BKV replication requires further elucidation.

Several studies have demonstrated that tacrolimus, mycophenolic acid or steroids substantially increases the risk of BKV replication when compared with CsA (41–44) but it is the net immunosuppressive status of the host that determines the development of PVAN. Although CsA can suppress BKV replication in the *in vitro* culture, the rationality of shifting to CsA-based immunosuppressants in renal transplant patients with PVAN still remains controversial due to side effects including nephrotoxicity and development of renal fibrosis (45). Since calcineurin/cyclophilin has functional diversity in regulating cell bio-functions and dephophorylates not only NFAT but also many intracellular proteins (17), CsA therefore blocks NFAT functionality as well as other important cell biological activities (46). Specific therapeutic agents targeting against CypA and NFAT may provide new potential anti-BKV treatment.

In conclusion, this study demonstrates an essential role of CypA and NFATc3 in BKV replication. CsA suppresses BKV replication through inhibition of CypA and NFAT functionalities.

Acknowledgments

Disclosure

The authors of this manuscript have no conflicts of interest to disclose as described by the *American Journal of Transplantation.*

References

1. Hirsch HH, Drachenberg CB, Steiger J, Ramos E. Polyomavirus-associated nephropathy in renal transplantation: Critical issues of screening and management. Adv Exp Med Biol 2006; 577: 160–173.

2. Li YJ, Chen YC, Lai PC, et al. A direct association of polyomavirus BK viruria with deterioration of renal allograft function in renal transplant patients. Clin Transplant 2009; 23: 505–510.

3. Hirsch HH, Brennan DC, Drachenberg CB, et al. Polyomavirus-associated nephropathy in renal transplantation: Interdisciplinary analyses and recommendations. Transplantation 2005; 79: 1277–1286.

4. BK virus. Am J Transplant 2004; 4(Suppl 10): 89–91.

5. Agha I, Brennan DC. BK virus and immunosuppressive agents. Adv Exp Med Biol 2006; 577: 174–184.

6. Brennan DC, Agha I, Bohl DL, et al. Incidence of BK with tacrolimus versus cyclosporine and impact of preemptive immunosuppression reduction. Am J Transplant 2005; 5: 582–594.

7. Franke EK, Luban J. Inhibition of HIV-1 replication by cyclosporine A or related compounds correlates with the ability to disrupt the Gag-cyclophilin A interaction. Virology 1996; 222: 279–282.

8. Damaso CR, Keller SJ. Cyclosporin A inhibits vaccinia virus replication in vitro. Arch Virol 1994; 134: 303–319.

9. Vahlne A, Larsson PA, Horal P, et al. Inhibition of herpes simplex virus production in vitro by cyclosporin A. Arch Virol 1992; 122: 61–75.

10. Wainberg MA, Dascal A, Blain N, et al. The effect of cyclosporine A on infection of susceptible cells by human immunodeficiency virus type 1. Blood 1988; 72: 1904–1910.

11. Kawasaki H, Mocarski ES, Kosugi I, Tsutsui Y. Cyclosporine inhibits mouse cytomegalovirus infection via a cyclophilin-dependent pathway specifically in neural stem/progenitor cells. J Virol 2007; 81: 9013–9023.

12. Watashi K, Hijikata M, Hosaka M, Yamaji M, Shimotohno K. Cyclosporin A suppresses replication of hepatitis C virus genome in cultured hepatocytes. Hepatology 2003; 38: 1282–1288.

13. Acott PD, O'Regan PA, Lee SH, Crocker JF. In vitro effect of cyclosporin A on primary and chronic BK polyoma virus infection in Vero E6 cells. Transpl Infect Dis 2008; 10: 385–390.

14. Li YJ, Weng CH, Lai WC, et al. A suppressive effect of cyclosporine A on replication and noncoding control region activation of polyomavirus BK virus. Transplantation 2010; 89: 299–306.

15. Handschumacher RE, Harding MW, Rice J, Drugge RJ, Speicher DW. Cyclophilin: A specific cytosolic binding protein for cyclosporin A. Science 1984; 226: 544–547.

16. Wang P, Heitman J. The cyclophilins. Genome Biol 2005; 6: 226.

17. Matsuda S, Koyasu S. Mechanisms of action of cyclosporine. Immunopharmacology 2000; 47: 119–125.

18. Ho S, Clipstone N, Timmermann L, et al. The mechanism of action of cyclosporin A and FK506. Clin Immunol Immunopathol 1996; 80(3 Pt 2): S40–S45.

19. Hogan PG, Chen L, Nardone J, Rao A. Transcriptional regulation by calcium, calcineurin, and NFAT. Genes Dev 2003; 17: 2205–2232.

20. Crabtree GR. Generic signals and specific outcomes: Signaling through Ca2+, calcineurin, and NF-AT. Cell 1999; 96: 611–614.

21. Chatterji U, Bobardt M, Selvarajah S, et al. The isomerase active site of cyclophilin A is critical for hepatitis C virus replication. J Biol Chem 2009; 284: 16998–17005.

22. Cron RQ, Bartz SR, Clausell A, Bort SJ, Klebanoff SJ, Lewis DB. NFAT1 enhances HIV-1 gene expression in primary human CD4 T cells. Clin Immunol 2000; 94: 179–191.

23. Tian YC, Chen YC, Chang CT, et al. Epidermal growth factor and transforming growth factor-beta1 enhance HK-2 cell migration through a synergistic increase of matrix metalloproteinase and sustained activation of ERK signaling pathway. Exp Cell Res 2007; 313: 2367–2377.

24. Goel M, Sinkins WG, Schilling WP. Selective association of TRPC channel subunits in rat brain synaptosomes. J Biol Chem 2002; 277: 48303–48310.

25. Tian YC, Hung CC, Li YJ, et al. Leptospira santorosai serovar shermani detergent extract induces an increase in fibronectin production through a toll-like receptor 2-mediated pathway. Infect Immun 2011; 79: 1134–1142.

26. Tian YC, Phillips AO. TGF-beta1-mediated inhibition of HK-2 cell migration. J Am Soc Nephrol 2003; 14: 631–640.

27. Moriyama T, Sorokin A. BK virus (BKV): Infection, propagation, quantitation, purification, labeling, and analysis of cell entry. Curr Protoc Cell Biol 2009;Chapter 26:Unit 26 2.

28. Watashi K, Ishii N, Hijikata M, et al. Cyclophilin B is a functional regulator of hepatitis C virus RNA polymerase. Mol Cell 2005; 19: 111–122.

29. Nakagawa M, Sakamoto N, Tanabe Y, et al. Suppression of hepatitis C virus replication by cyclosporin a is mediated by blockade of cyclophilins. Gastroenterology 2005; 129: 1031–1041.

30. Jain J, McCaffrey PG, Miner Z, et al. The T-cell transcription factor NFATp is a substrate for calcineurin and interacts with Fos and Jun. Nature 1993; 365: 352–355.

31. Martinez-Martinez S, Redondo JM. Inhibitors of the calcineurin/NFAT pathway. Curr Med Chem 2004; 11: 997–1007.

32. Liu S, Asparuhova M, Brondani V, Ziekau I, Klimkait T, Schumperli D. Inhibition of HIV-1 multiplication by antisense U7 snRNAs and siRNAs targeting cyclophilin A. Nucleic Acids Res 2004; 32: 3752–3759.

33. Chatterji U, Bobardt M, Lim P, Gallay P. Cyclophilin A-Independent Recruitment of NS5A and NS5B Into HCV Replication Complexes. J Gen Virol 2010; 91: 1189–1193.

34. Kaul A, Stauffer S, Berger C, et al. Essential role of cyclophilin A for hepatitis C virus replication and virus production and possible link to polyprotein cleavage kinetics. PLoS Pathog 2009; 5: e1000546.

35. Yang F, Robotham JM, Nelson HB, Irsigler A, Kenworthy R, Tang H. Cyclophilin A is an essential cofactor for hepatitis C virus infection and the principal mediator of cyclosporine resistance in vitro. J Virol 2008; 82: 5269–5278.

36. Jordan JA, Manley K, Dugan AS, O'Hara BA, Atwood WJ. Transcriptional regulation of BK virus by nuclear factor of activated T cells. J Virol 2010; 84: 1722–1730.

37. Romanchikova N, Ivanova V, Scheller C, Jankevics E, Jassoy C, Serfling E. NFAT transcription factors control HIV-1 expression through a binding site downstream of TAR region. Immunobiology 2003; 208: 361–365.

38. Manley K, O'Hara B A, Gee GV, Simkevich CP, Sedivy JM, Atwood WJ. NFAT4 is required for JC virus infection of glial cells. J Virol 2006; 80: 12079–12085.

39. Trevillyan JM, Chiou XG, Chen YW, et al. Potent inhibition of NFAT activation and T cell cytokine production by novel low molecular weight pyrazole compounds. J Biol Chem 2001; 276: 48118–48126.

40. Sundsfjord A, Johansen T, Flaegstad T, et al. At least two types of control regions can be found among naturally occurring BK virus strains. J Virol 1990; 64: 3864–3871.

41. Barri YM, Ahmad I, Ketel BL, et al. Polyoma viral infection in renal transplantation: The role of immunosuppressive therapy. Clin Transplant 2001; 15: 240–246.

42. Binet I, Nickeleit V, Hirsch HH, et al. Polyomavirus disease under new immunosuppressive drugs: A cause of renal graft dysfunction and graft loss. Transplantation 1999; 67: 918–922.

43. Dadhania D, Snopkowski C, Ding R, et al. Epidemiology of BK virus in renal allograft recipients: Independent risk factors for BK virus replication. Transplantation 2008; 86: 521–528.

44. Nickeleit V, Hirsch HH, Binet IF, et al. Polyomavirus infection of renal allograft recipients: From latent infection to manifest disease. J Am Soc Nephrol 1999; 10: 1080–1089.

45. Chapman JR, Nankivell BJ. Nephrotoxicity of ciclosporin A: Short-term gain, long-term pain? Nephrol Dial Transplant 2006; 21: 2060–2063.

46. Akool el S, Doller A, Babelova A, et al. Molecular mechanisms of TGF beta receptor-triggered signaling cascades rapidly induced by the calcineurin inhibitors cyclosporin A and FK506. J Immunol 2008; 181: 2831–2845.

Identification of Novel *N*-(Morpholine-4-Carbonyloxy) Amidine Compounds as Potent Inhibitors against Hepatitis C Virus Replication

Akiko Kusano-Kitazume, Naoya Sakamoto, Yukiko Okuno, Yuko Sekine-Osajima, Mina Nakagawa, Sei Kakinuma, Kei Kiyohashi, Sayuri Nitta, Miyako Murakawa, Seishin Azuma, Yuki Nishimura-Sakurai, Masatoshi Hagiwara and Mamoru Watanabe

Identification of Novel N-(Morpholine-4-Carbonyloxy) Amidine Compounds as Potent Inhibitors against Hepatitis C Virus Replication

Akiko Kusano-Kitazume,[a] Naoya Sakamoto,[a,b] Yukiko Okuno,[c] Yuko Sekine-Osajima,[a] Mina Nakagawa,[a,b] Sei Kakinuma,[a,b] Kei Kiyohashi,[a] Sayuri Nitta,[a] Miyako Murakawa,[a] Seishin Azuma,[a] Yuki Nishimura-Sakurai,[a] Masatoshi Hagiwara,[c] and Mamoru Watanabe[a]

Department of Gastroenterology and Hepatology[a] and Department for Hepatitis Control,[b] Tokyo Medical and Dental University, Tokyo, Japan, and Department of Anatomy and Developmental Biology, Graduate School of Medicine, Kyoto University, Kyoto, Japan[c]

To identify novel compounds that possess antiviral activity against hepatitis C virus (HCV), we screened a library of small molecules with various amounts of structural diversity using an HCV replicon-expressing cell line and performed additional validations using the HCV-JFH1 infectious-virus cell culture. Of 4,004 chemical compounds, we identified 4 novel compounds that suppressed HCV replication with 50% effective concentrations of ranging from 0.36 to 4.81 μM. N'-(Morpholine-4-carbonyloxy)-2-(naphthalen-1-yl) acetimidamide (MCNA) was the most potent and also produced a small synergistic effect when used in combination with alpha interferon. Structure-activity relationship (SAR) analyses revealed 4 derivative compounds with antiviral activity. Further SAR analyses revealed that the N-(morpholine-4-carbonyloxy) amidine moiety was a key structural element for antiviral activity. Treatment of cells with MCNA activated nuclear factor κB and downstream gene expression. In conclusion, N-(morpholine-4-carbonyloxy) amidine and other related morpholine compounds specifically suppressed HCV replication and may have potential as novel chemotherapeutic agents.

epatitis C virus (HCV) is a major human pathogen. It is associated with persistent liver infection, which leads to the development of chronic hepatitis, liver cirrhosis, and hepatocellular carcinoma (13). Treatment with pegylated interferon (IFN) and ribavirin is associated with significant side effects and is effective in only half the patients infected with HCV genotype 1 (6). More effective and more tolerable therapeutics are under development, and direct-acting antiviral agents (DAAs) for HCV infection are currently in advanced clinical trials. In combination with IFN and ribavirin, the HCV protease inhibitors telaprevir and boceprevir have recently been approved for treatment of genotype 1 HCV infection in the United States, Canada, Europe, and Asian countries (11, 12, 22). Although these two drugs can achieve higher sustained virologic response rates than IFN and ribavirin, their effects could be compromised by the emergence of highly prevalent drug-resistant mutants (25). Thus, it is crucial to use several different classes of DAAs in combination to improve efficacy and reduce viral breakthrough.

The HCV subgenomic replicon system has been widely used to screen compound libraries for inhibitors of viral replication, using reporter activity as a surrogate marker for HCV replication. We previously reported the successful adaptation of the Huh7/Rep-Feo replicon cell line to a high-throughput screening assay system (28). This approach contributed to the discovery of antiviral compounds, such as hydroxyl-methyl-glutaryl coenzyme A reductase inhibitors (10) and epoxide compounds (20). In our present study, we used the Huh7/Rep-Feo replicon cell line to screen a library of small molecules with various amounts of structural diversity to identify novel compounds possessing antiviral activity against HCV. We showed that the screening hit compounds inhibited HCV replication in an HCV genotype 2a (JFH-1) infectious-virus cell culture (29). The most potent compound was N'-(morpholine-4-carbonyloxy)-2-(naphthalen-1-yl) acetimidamide (MCNA). Structure-activity relationship (SAR) analyses revealed that the N-(morpholine-4-carbonyloxy) amidine moiety

was a key structural element for antiviral activity. We also investigated the possible mechanisms of action of these compounds and showed that MCNA likely inhibited HCV replication through activation of the nuclear factor κB (NF-κB) pathway.

MATERIALS AND METHODS

Reagents and chemicals. Recombinant human alpha 2b interferon (IFN-α2b) was obtained from Schering-Plough (Kenilworth, NJ), the NS3/4A protease inhibitor BILN 2061 from Boehringer Ingelheim (Ingelheim, Germany), beta-mercaptoethanol from Wako (Osaka, Japan), and recombinant human tumor necrosis factor alpha (TNF-α) from Sigma (St. Louis, MO). The library of chemicals that were screened was provided by the Chemical Biology Screening Center at Tokyo Medical and Dental University. Information about the library is available at http://bsmdb.tmd .ac.jp. The important features of the library were the abundance of pharmacophores and the great diversity. Lipinski's rule of five was used to evaluate drug similarity (15). The purity of each chemical from the library was greater than 90%. For SAR analyses, 27 compounds were purchased from Assinex (Moscow, Russia), ChemBridge (San Diego, CA), ChemDiv (San Diego, CA), Enamine (Kiev, Ukraine), Maybridge (Cambridge, United Kingdom), Ramidus AB (Lund, Sweden), SALOR (St. Louis, MO), Scientific Exchange (Center Ossipee, NH), or Vitas-M (Moscow, Russia). The chemicals were all prepared at concentrations of 10 mM in dimethyl sulfoxide (Sigma) and stored at −20°C until they were used.

Cell lines and cell culture maintenance. Huh7 and Huh7.5.1 cell lines (32) were maintained in Dulbecco's modified Eagle's medium (Sigma)

supplemented with 10% fetal bovine serum and incubated at 37°C under 5% CO_2. The maintenance medium for the HCV replicon-harboring cell line, Huh7/Rep-Feo, was supplemented with 500 μg/ml of G418 (Nacalai Tesque, Kyoto, Japan).

HCV replicon construction and cell culture. An HCV subgenomic replicon plasmid that contained Rep-Feo, pHC1bneo/delS (Rep-Feo-1b), was derived from the HCV-N strain. RNA was synthesized from pRep-Feo and transfected into Huh7 cells. After culture in the presence of G418, a cell line that stably expressed the replicon was established (28, 31).

Cell-based screening of antiviral activity. Huh7/Rep-Feo cells were seeded at a density of 4,000 cells/well in 100 μl of medium in 96-well plates and incubated for 24 h. Test compound solutions, 10 mM in 100% dimethyl sulfoxide (DMSO), were added to the wells; for primary screening, the final concentration was 5 μM. The assay plates were incubated as described above for another 48 h, and luciferase activity was measured with a luminometer (Perkin-Elmer) using the Bright-Glo Luciferase assay system (Promega) following the manufacturer's instructions. Assays were performed in triplicate, and the results were expressed as means and standard deviations (SD) as percentages of the controls. Compounds were considered hits if they inhibited >50% of the mean control luciferase activities. Compounds were considered cytotoxic if they reduced cell viability below 70% of the control in dimethylthiazol carboxymethoxyphenyl sulfophenyl tetrazolium (MTS) assays and were discarded. The hit compounds were then validated by secondary screening, which determined the antiviral activities of each compound serially diluted at concentrations ranging from 0.1 μM to 30 μM under Huh7/Rep-Feo cells cultured in an identical manner to the primary screen. Compounds inhibiting replication with a 50% effective concentration (EC_{50}) of <5 μM and a selectivity index (SI) of >5 were selected for further analysis.

MTS assay. To evaluate cell viability, MTS assays were performed using the CellTiter 96 Aqueous One Solution Cell Proliferation Assay (Promega) according to the manufacturer's directions.

Calculation of the EC_{50}, CC_{50}, and SI. The EC_{50} indicates the concentration of test compound that inhibits replicon-based luciferase activity by 50%. The 50% cytotoxic concentration (CC_{50}) indicates the concentration that inhibits cell viability by 50%. The EC_{50} and CC_{50} values were calculated using probit regression analysis (2, 26). The selectivity index was calculated by dividing the CC_{50} by the EC_{50}.

Reporter and expression plasmids. The plasmid pC1neo-Rluc-IRES-Fluc was constructed to analyze the HCV internal ribosome entry site (IRES)-mediated translation efficiency (19). The plasmid expressed a bicistronic mRNA containing the *Renilla* luciferase gene translated in a cap-dependent manner, and firefly luciferase was translated by HCV-IRES-mediated initiation. The plasmid pISRE-TA-Luc (Invitrogen, Carlsbad, CA) expressed the firefly luciferase reporter gene under the control of the interferon stimulation response element (ISRE). The plasmid pNF-κB-TA-Luc (Clontech Laboratories, Franklin Lakes, NJ) expressed the firefly luciferase reporter gene under the control of NF-κB. The plasmid pRL-CMV (Promega, Madison, WI), which expressed the *Renilla* luciferase gene under the control of the cytomegalovirus early promoter/enhancer, was used as a control for the transfection efficiency of pISRE-TA-Luc and pNF-κB-TA-Luc (8).

Western blot analysis. Fifteen micrograms of total cell lysates was separated using NuPage 4-to-12% Bis-Tris gels (Invitrogen) and blotted onto polyvinylidene difluoride membranes. Each membrane was incubated with primary antibodies followed by a peroxidase-labeled anti-IgG antibody and visualized by chemiluminescence reaction using the ECL Western Blotting Analysis System (Amersham Biosciences, Buckinghamshire, United Kingdom). The primary antibodies were anti-NS5A (BioDesign, Saco, ME), anti-HCV core (kindly provided by T. Wakita), anti-phospho-p65 (Ser536) (93H1; Cell Signaling Technology, Beverly, MA), anti-IκBα (Santa Cruz Biotechnology, Santa Cruz, CA), and anti-β-actin (Sigma) antibodies.

HCV-JFH1 virus cell culture. HCV-JFH1 RNA transcribed *in vitro* was transfected into Huh7.5.1 cells. The transfected cells were subcultured

TABLE 1 Effects of the leading hit compounds on HCV replication[a]

Compound	EC_{50} (μM)	CC_{50} (μM)	SI
1	0.36 (0.22–0.58)	45.2 (35.9–56.9)	126
2	0.86 (0.73–1.02)	>100	>116
3	0.94 (0.76–1.06)	25.3 (19.8–32.3)	26.9
4	4.81 (3.79–6.12)	27.1 (17.1–58.0)	5.64

[a] The EC_{50} and CC_{50} values are reported, with 95% confidence intervals in parentheses, from a representative experiment performed in triplicate.

every 3 to 5 days. The culture supernatant was subsequently transferred onto Huh7.5.1 cells.

Real-time RT-PCR analysis. The protocols and primers for real-time RT-PCR analysis of HCV RNA have been described previously (17). Briefly, total cellular RNA was isolated using an RNeasy Minikit (Qiagen, Valencia, CA), reverse transcribed, and subjected to real-time RT-PCR analysis. Expression of mRNA was quantified using the TaqMan Universal PCR Master Mix (Applied Biosystems, Foster City, CA) and the ABI 7500 real-time PCR system (Applied Biosystems).

Analyses of drug synergism. The effects on HCV replication of antiviral hit compounds plus IFN-α or BILN 2061 were analyzed according to classical isobologram analyses (24, 28). Dose-inhibition curves for IFN or BILN 2061 and the test compounds were drawn, with the 2 drugs (IFN or BILN 2061 and each test compound) used alone or in combination. For each drug combination, the concentrations of IFN or BILN 2061 and test compound that inhibited HCV replication by 50% (EC_{50}s) were plotted against the fractional concentration of IFN or BILN 2061 and the compound on the x and y axes, respectively. A theoretical line of additivity was drawn between plots of the EC_{50}s obtained for either drug used alone. The combined effects of the 2 drugs were considered to be additive, synergistic, or antagonistic if the plots of the combined drugs were located on, below, or above the line of additivity, respectively.

Statistical analyses. Statistical analyses were performed using Welch's t test. P values of less than 0.01 were considered statistically significant.

RESULTS

Screening results. To identify novel regulators of HCV replication, 4,004 chemical compounds were screened using the Huh7/Rep-Feo replicon assay system. The primary screens identified 117 compounds that inhibited ≥50% of replicon luciferase activity at 5 μM. Of the 117 compounds, 74 were cytotoxic and could not be further evaluated. In the secondary screen, nontoxic primary hits were evaluated by determining the antiviral activities of serial dilutions at concentrations ranging from 0.1 μM to 30 μM. This screen identified 19 compounds with EC_{50}s of less than 5 μM and CC_{50} values 5-fold greater than the EC_{50} values. The effect of each secondary hit on HCV-NS5A protein expression was examined using Western blot analysis. Of the 19 compounds, 4 compounds, designated 1, 2, 3, and 4, suppressed HCV subgenomic replication, with EC_{50}s ranging from 0.36 to 4.81 μM and SIs ranging from 5.64 to more than 100 (Table 1 and Fig. 1A and B; see Table S1 in the supplemental material). By Western blot analysis, compounds 1, 2, and 3 decreased HCV-NS5A protein levels at concentrations of 5 μM after incubation for 48 h (Fig. 1C). Compared with compounds 1, 2, and 3, the effect of compound 4 on HCV-NS5A protein expression was not remarkable at a concentration of 5 μM, similar to the results from the luciferase assay shown in Fig. 1B. The effects of the compounds on the HCV replicon were further validated in the JFH-1 cell culture. As shown in Fig. 1D, compounds 1, 2, 3, and 4 significantly inhibited intracellular RNA replication of HCV-JFH1. Although compound 4 was negative by Western blot analysis, it decreased HCV replication in the other
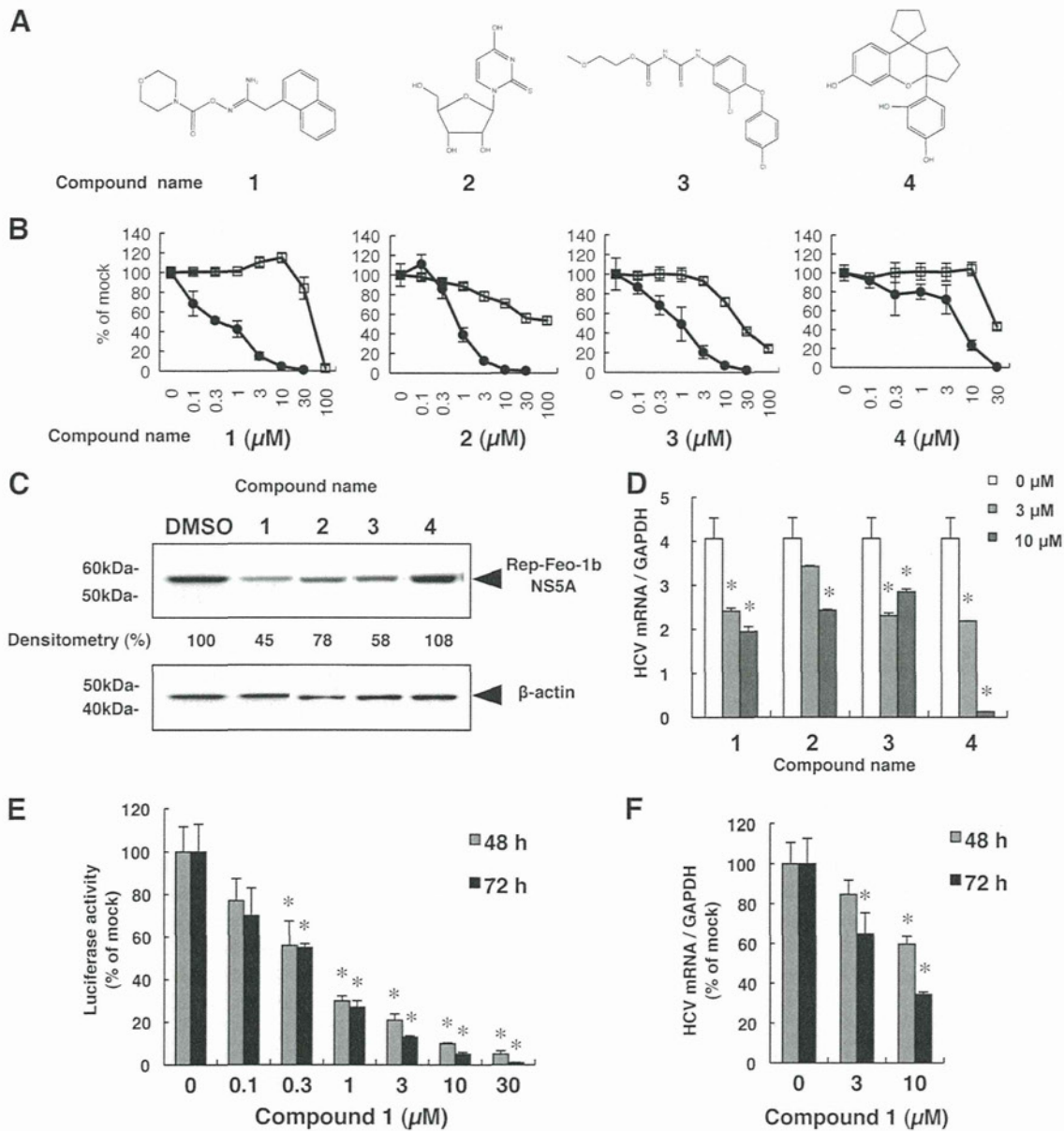
FIG 1 Effects of 4 screening hit compounds on HCV replication. (A) Chemical structures of hit compounds. (B) Huh7/Rep-Feo cells were treated with the indicated concentration of each compound for 48 h. Luciferase activities representing HCV replication are shown as percentages of the DMSO-treated control luciferase activity (solid circles). Cell viability is shown as a percentage of control viability (open squares). Each point represents the mean of triplicate data points, with the standard deviations represented as error bars. (C) Huh7/Rep-Feo cells were treated with DMSO or compounds 1 through 4 at 5 μM for 48 h, and Western blotting was performed using anti-HCV NS5A and anti-β-actin antibodies. Densitometry of NS5A protein was performed, and the results are indicated as percentages of the DMSO-treated control. The assay was repeated three times, and a representative result is shown. (D) Huh7.5.1 cells were transfected with HCV-JFH1 RNA and cultured in the presence of the indicated compounds at 3 μM or 10 μM. At 72 h after transfection, the cellular expression levels of HCV-RNA were quantified by real-time RT-PCR. The bars indicate means and SD. (E) Time-dependent reduction of luciferase activities in Huh7/Rep-Feo cells induced by compound 1. Luciferase activities are shown as percentages of the DMSO-treated control luciferase activity. The bars indicate means and SD. (F) Time-dependent reduction of cellular expression levels of HCV-RNA in HCV-JFH1-transfected cells induced by compound 1. HCV RNA levels are shown as percentages of the DMSO-treated control HCV-RNA level. The bars indicate means and SD. The asterisks indicate P values of less than 0.01.

assays, including the replicon and HCV-JFH1 virus assays. Thus, we concluded that compound 4 was an antiviral hit. These results indicated that the 4 compounds identified by cell-based screening suppressed subgenomic HCV replication and HCV replication in an HCV-based cell culture.

Hit compounds did not suppress HCV IRES-mediated translation. To determine whether the leading antiviral hits suppressed HCV IRES-dependent translation, we used the Huh7 cell line that had been stably transfected with pCIneo-Rluc IRES-Fluc. Treatment of these cells with the test compounds did not result in significant change in the internal luciferase activities at compound concentrations that suppressed expression of the HCV replicon (Fig. 2), suggesting that the effect of the hit compounds on HCV replication does not involve suppression of IRES-mediated viral-protein synthesis.
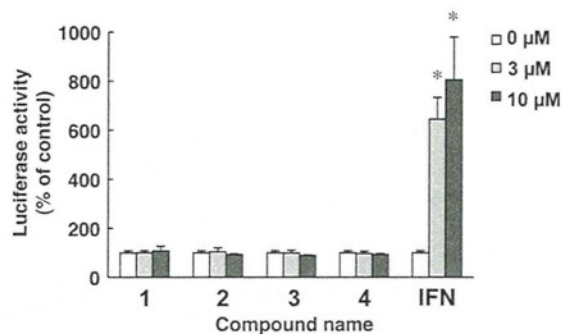
- 593 -
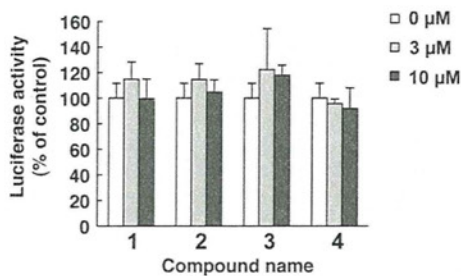
FIG 2 Hit compounds do not affect HCV IRES-mediated translation. The bicistronic reporter plasmid pC1neo-Rluc-IRES-Fluc was transfected into Huh7 cells. The cells were cultured in the presence of the indicated concentrations of compounds 1 through 4. After 6 h of treatment, luciferase activities were measured, and the values were normalized against *Renilla* luciferase activities. The assays were performed in triplicate. The bars indicate means and SD.

FIG 3 Hit compounds do not activate interferon-stimulated gene responses. Plasmids pISRE-TA-Luc and pRL-CMV were cotransfected into Huh7 cells. The transfected cells were cultured in the presence of the indicated concentrations of the hit compounds. After 6 h of treatment, luciferase activities were measured, and the values were normalized against *Renilla* luciferase activities. As positive controls, cells were treated with IFN-α at a concentration of 0, 3, or 10 U/ml. The bars indicate means and SD. The asterisks indicate *P* values of less than 0.01.

Hit compounds do not activate interferon-stimulated gene responses. To study whether the actions of the hit compounds involved IFN-mediated antiviral signaling that would induce expression of an IFN-stimulated gene, an ISRE-luciferase reporter plasmid, pISRE-TA-Luc, was transfected into Huh7 cells, and the transfected cells were cultured in the presence of the 4 compounds at concentrations of 0, 3, or 10 μM. In contrast to interferon, which elevated ISRE promoter activities significantly, the hit compounds showed no effects on the ISRE-luciferase activities (Fig. 3). These results indicated that the action of the hit compounds is independent of interferon signaling.

Drug synergism with IFN-α or BILN 2061. To investigate whether the hit compounds were synergistic with IFN-α or the protease inhibitor BILN 2061, we used isobologram analyses (24, 28). HCV replicon cells were treated with a combination of IFN-α or BILN 2061 and each hit compound at an EC$_{50}$ ratio of 1:0, 4:1, 3:2, 2:3, 1:4, or 0:1, and the dose-effect results were plotted (Fig. 4A and C). The fractional EC$_{50}$s for IFN-α or BILN 2061 and each compound were plotted on the *x* and *y* axes, respectively, to generate an isobologram. As shown in Fig. 4B, all plots of the fractional EC$_{50}$s of compound 1 and IFN-α fell below the line of additivity, while the plots were located closed to the line of additivity for the treatments using IFN-α plus compound 2 or 3 and above the line for the treatment using IFN-α plus compound 4. Those results indicated that the anti-HCV effect of compound 1 was synergistic with IFN-α, the anti-HCV effects of compounds 2 and 3 were additive, and the effect of compound 4 was antagonistic. In the BILN 2061 combination study, the combination with compound 2 was slightly synergistic, while the combination with compound 1 or 3 was additive, and the combination with compound 4 was antagonistic (Fig. 4D).

SARs of compound 1 and similar compounds. We next conducted SAR analyses for hit compound 1 by screening 69 compounds with structures similar to that of compound 1 (see Table S2 in the supplemental material). Out of those compounds, we identified 4 structural analogues that suppressed subgenomic HCV replication with EC$_{50}$s ranging from 1.82 to 4.03 μM and SIs of 6.01 through >43.7 (Table 2 and Fig. 5A and B). Similarly, the 4 compounds designated 5, 6, 7, and 8 substantially decreased HCV-NS5A protein expression levels following treatment with the compounds (Fig. 5C). Consistent with the replicon results, the compounds significantly suppressed HCV-JFH1 mRNA in cell

culture (Fig. 5D). Although the suppressive activities of the 4 compounds were similar, the original compound 1 showed the greatest anti-HCV activity. Therefore, we conducted SAR analyses of the compound 1 *N*-(morpholine-4-carbonyloxy) amidine and *N*-acyloxy-1-naphthalenacetamidine moieties. We screened 13 compounds containing *N*-(morpholine-4-carbonyloxy) amidine and 11 with *N*-acyloxy-1-naphthalenacetamidine (Fig. 6A; see Table S3 in the supplemental material). Intriguingly, 11 out of the 13 *N*-(morpholine-4-carbonyloxy) amidine compounds suppressed the subgenomic HCV replicon without cytotoxicity at a fixed concentration of 5 μM. In contrast, only 2 *N*-acyloxy-1-naphthalenacetamidine compounds decreased HCV replication (Fig. 6B and C). We also conducted dose-dependent suppression assays for HCV replicon. As shown in Table 3, 11 out of 13 *N*-(morpholine-4-carbonyloxy) amidine compounds consistently decreased subgenomic HCV replication, with EC$_{50}$s ranging from 1.52 through 8.62 μM and SIs of 14.2 to >61.4. Of these 11 compounds, compound 14 was the most potent, with an EC$_{50}$ of 1.63 μM and an SI of >61.4. The antiviral effect of compound 14 against HCV-JFH1 was identical to that of the original compound 1. To identify the moiety conferring anti-HCV activity, we tested the morpholine-4-carboxyl moiety within the *N*-(morpholine-4-carboynloxy) amidine structure (Fig. 6D). Three compounds bearing the morpholine-4-carboxyl moiety were tested, and none showed suppressive activity toward the HCV replicon. These results suggested that the entire *N*-(morpholine-4-carbonyloxy) amidine moiety was important for efficient anti-HCV activity.

Effect of compound 1 on the NF-κB signaling pathway. NF-κB, composed of homo- and heterodimeric complexes of Rel-like domain-containing proteins, including p50 and p65, is a key regulator of innate and adaptive immune responses through transcriptional activation of several antiviral proteins (9, 23). We performed luciferase reporter assays, a p65 phosphorylation assay, and an IκB-α degradation assay to assess the effect of compound 1 on NF-κB signaling in host cells. Intriguingly, treatment of both Huh7 cells and HCV replicon-expressing cells with compound 1 increased NF-κB reporter activity in a dose-dependent manner (Fig. 7A and B). Consistently, treatment with compound 1 increased phosphorylated NF-κB p65 in Huh7 cells (Fig. 7C). Acti-